

AD-A112 031

SHAKER RESEARCH CORP BALLSTON LAKE NY
DEVELOPMENT OF A LUBRICANT TRACTION MEASURING DEVICE, (U)
SEP 81 R L SMITH

F/6 11/8

F33615-79-C-5051

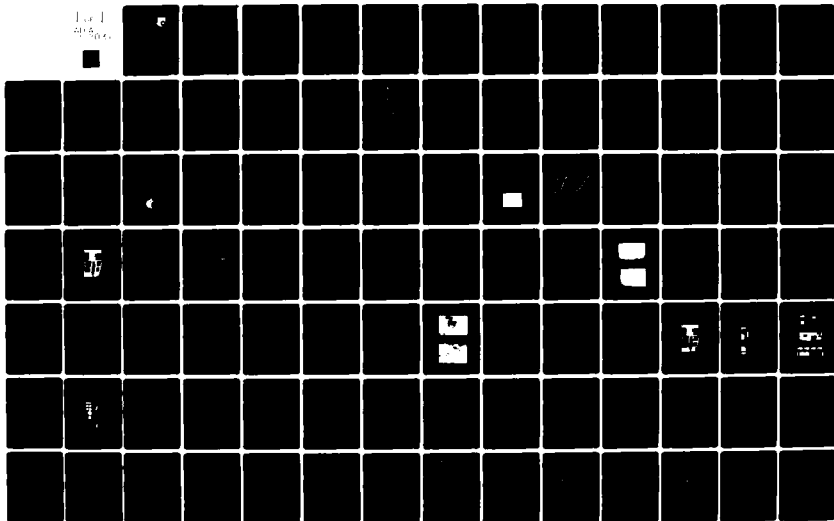
UNCLASSIFIED

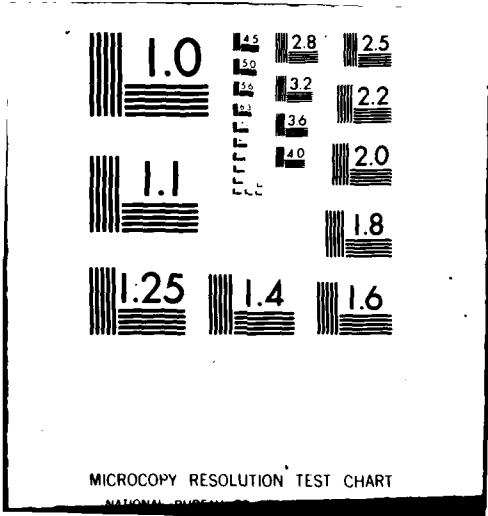
SRC81-TR-73

AFWAL-TR-81-4102

NL

1 of 1
4/6/81





MICROCOPY RESOLUTION TEST CHART

NATIONAL BUREAU OF STANDARDS-1963-A

12

ADA112031

AFWAL-TR-81-4102



DEVELOPMENT OF A LUBRICANT TRACTION MEASURING DEVICE

R. L. Smith

SHAKER RESEARCH CORPORATION
BALLSTON LAKE, NEW YORK 12019

September 1981

Final Report for Period July 1979 - September 1981

Approved for public release; distribution unlimited

DTIC FILE COPY

MATERIALS LABORATORY
AIR FORCE WRIGHT AERONAUTICAL LABORATORIES
AIR FORCE SYSTEMS COMMAND
WRIGHT-PATTERSON AIR FORCE BASE, OHIO 45433

DTIC
MAR 16 1982
H

82 08 1 007

NOTICE

When Government drawings, specifications, or other data are used for any purpose other than in connection with a definitely related Government procurement operation, the United States Government thereby incurs no responsibility nor any obligation whatsoever; and the fact that the government may have formulated, furnished, or in any way supplied the said drawings, specifications, or other data, is not to be regarded by implication or otherwise as in any manner licensing the holder or any other person or corporation, or conveying any rights or permission to manufacture, use, or sell any patented invention that may in any way be related thereto.

This report has been reviewed by the Office of Public Affairs (ASD/PA) and is releasable to the National Technical Information Service (NTIS). At NTIS, it will be available to the general public, including foreign nations.

This technical report has been reviewed and is approved for publication.

Howard E Bandow

HOWARD E. BANDOW
Project Monitor

B. D. McConnell

B. D. McCONNELL
Acting Chief, Fluids,
Lubricants, and Elastomers Branch

FOR THE COMMANDER

F. D. Cherry

FRANKLIN D. CHERRY, Chief
Nonmetallic Materials Division

"If your address has changed, if you wish to be removed from our mailing list, or if the addressee is no longer employed by your organization please notify AFWAL/MLBT, W-PAFB, OH 45433 to help us maintain a current mailing list."

Copies of this report should not be returned unless return is required by security considerations, contractual obligations, or notice on a specific document.

UNCLASSIFIED

SECURITY CLASSIFICATION OF THIS PAGE (When Data Entered)

REPORT DOCUMENTATION PAGE		READ INSTRUCTIONS BEFORE COMPLETING FORM								
1. REPORT NUMBER AFWAL-TR-81-4102	2. GOVT ACCESSION NO. AD-A223 032	3. RECIPIENT'S CATALOG NUMBER								
4. TITLE (and Subtitle) DEVELOPMENT OF A LUBRICANT TRACTION MEASURING DEVICE	5. TYPE OF REPORT & PERIOD COVERED Final Report July 1979 - September 1981									
	6. PERFORMING ORG. REPORT NUMBER SRC81-TR-73									
7. AUTHOR(s) Richard L. Smith	8. CONTRACT OR GRANT NUMBER(s) F33615-79-C-5051									
9. PERFORMING ORGANIZATION NAME AND ADDRESS Shaker Research Corporation Northway 10 Executive Park Ballston Lake, NY 12019	10. PROGRAM ELEMENT, PROJECT, TASK AREA & WORK UNIT NUMBERS 24210206									
11. CONTROLLING OFFICE NAME AND ADDRESS Materials Laboratory (MLBT) Air Force Wright Aeronautical Laboratories Air Force Systems Command Wright-Patterson Air Force Base, OH 45433	12. REPORT DATE September 1981									
	13. NUMBER OF PAGES									
14. MONITORING AGENCY NAME & ADDRESS (if different from Controlling Office)	15. SECURITY CLASS. (of this report) Unclassified									
	15a. DECLASSIFICATION/DOWNGRADING SCHEDULE									
16. DISTRIBUTION STATEMENT (of this Report) Approved for public release; distribution unlimited.										
17. DISTRIBUTION STATEMENT (of the abstract entered in Block 20, if different from Report)										
18. SUPPLEMENTARY NOTES										
19. KEY WORDS (Continue on reverse side if necessary and identify by block number)										
<table border="0"> <tr> <td>Elastohydrodynamic lubrication</td> <td>Asperity Interactions</td> </tr> <tr> <td>Traction</td> <td>Viscosity</td> </tr> <tr> <td>Film Thickness</td> <td>Capacitance</td> </tr> <tr> <td>Rolling Disc Machine</td> <td>Contact Resistance</td> </tr> </table>			Elastohydrodynamic lubrication	Asperity Interactions	Traction	Viscosity	Film Thickness	Capacitance	Rolling Disc Machine	Contact Resistance
Elastohydrodynamic lubrication	Asperity Interactions									
Traction	Viscosity									
Film Thickness	Capacitance									
Rolling Disc Machine	Contact Resistance									
20. ABSTRACT (Continue on reverse side if necessary and identify by block number)										
<p>The primary objectives of this research program were to design, develop, and fabricate a traction measuring apparatus. As designed, this device makes use of small quantities of lubricant for traction evaluation. One candidate fluid was placed in the test rig for evaluation purposes during the project. A set of sample performance data was gathered on this fluid for testing of the rig.</p>										

UNCLASSIFIED

SECURITY CLASSIFICATION OF THIS PAGE(When Data Entered)

20. (continued)

The constructed traction apparatus described in this report consists of a mechanical assembly and separate instrumentation panel. The mechanical assembly contains the drive motors (two 10 H.P. units), the belted transmissions, the assembly shafting, and all the support structural hardware. The instrumentation panel is for controlling and monitoring the test operations. These two units can be placed separately for the convenience of testing.

Accession For	
NTIS CR&I	<input checked="" type="checkbox"/>
DTIC T	<input type="checkbox"/>
Unannounced	<input type="checkbox"/>
Justification	
By _____	
Distribution/	
Availability Codes	
Dist	Avail and/or
	Special



UNCLASSIFIED

SECURITY CLASSIFICATION OF THIS PAGE(When Data Entered)

FOREWORD

This report was prepared at Shaker Research Corporation, Ballston Lake, New York, under USAF Contract No. F33615-79-C-5051. The work was initially administered under the technical direction of Mr. Fred Brooks. In the final phases the work was monitored by Dr. Howard Bandow. These project engineers directed this effort, which covers the period from July 1979 through September 1981, while at the Materials Laboratory, Air Force Wright Aeronautical Laboratories, Wright-Patterson Air Force Base, Ohio.

TABLE OF CONTENTS

	<u>Page</u>
I INTRODUCTORY SUMMARY AND CONCLUSION _____	1
II TECHNICAL DISCUSSION _____	6
1. Traction Measurement _____	8
2. State-of-the-Art Traction Rig Design _____	13
a. Test Disk Geometric Considerations _____	13
b. Test Disk Inertial Considerations _____	15
c. Torque Sensing _____	16
d. Rolling and Slip Speeds _____	17
e. Lubricant Temperature _____	19
f. Lubricated Contact Loading _____	23
g. Film Condition Monitoring _____	25
h. Vibration Detection _____	28
3. Description of the Design _____	28
a. Description of Overall Arrangement _____	28
b. Drive System _____	32
c. Test Disk Support Spindles _____	38
d. Loading Mechanism _____	42
e. Test Disk Enclosure and Lubricant Circulating System _____	45
f. Drive Motors _____	47
g. Instrumentation for Data Monitoring _____	49
h. Control Panel Layout _____	53
REFERENCES _____	59
APPENDIX I Traction Apparatus Design Drawings List _____	62
APPENDIX II List of Instrumentation Monitoring Equipment _____	68
APPENDIX III Sample Data Scanner Program Listing _____	70
APPENDIX IV Physical Properties of Fluid O-77-3J Lubricant Used in this Investigation _____	72
APPENDIX V Sample Traction vs. Slip Speed Data _____	75

LIST OF ILLUSTRATIONS

	<u>Page</u>
1. Traction Rig Features _____	2
2. Simple Two Disk Design for the Study of Lubricant Characteristics _____	3
3. Tractive Forces in a Lubricated Contact as a Function of Contact Surface Sliding Speeds _____	9
4. Traction Data from Rolling Disk Rig with Four Separate Normal Loads _____	10
5. Difference between Traction Curves of Polyphenyl Ether and MIL-L-7808 _____	12
6. Traction Apparatus with Undesirable Hertzian Contact Zone Arrangement _____	14
7. Sample Shaft Speed Timing Signal Output and Detection _____	20
8. Affect of Lubricant Inlet Temperature on Traction Characteristic _____	21
9. Electrical Contact Diagram and Contact Resistance Signal _____	26
10. Asperity Contact Load/Level Sensitivity _____	27
11. Plan View of Traction Apparatus _____	29
12. General Assembly _____	30
13. Drawing of Control and Instrument Panel _____	31
14. Test Room Layout _____	33
15. Maximum Attainable Traction Coefficients for 1.125 inch Diameter Test Disks _____	35
16. Support Spindle Assembly _____	36
17. Drive Transmission Torque Limits _____	37
18. High Speed Test Disk Support Shaft _____	39
19. Test Spindle Schematic _____	41
20. Schematic of Test Disk Enclosure _____	46
21. Transmission Shafting _____	50
22. Rig Wiring Requirements _____	51
23. Instrument Control and Monitor Panels _____	54
24. Instrument Monitors for Load, Slip Speed, Displacement, and Acceleration _____	55

	<u>Page</u>
25. Instrument Monitors for Temperature, Electric Contact Torque (Traction), and Data Logging (Full Right Side View of Instrument Panel) _____	56
26. Sample Data Logger Printout _____	57
27. Control Panel Layout Details _____	58

LIST OF TABLES

	<u>Page</u>
1. Contributions to Elastohydrodynamic Lubrication Technology_____	7
2. Comparison of Three Types of Rotating Shaft Torque Sensors_____	18
3. Hertzian Stresses for Various Disk Normal Loads (Heavy Loads)_____	24
4. Summary Table of Spindle Stresses_____	42
5. Critical Speed Analysis Summary_____	44
6. Small Traction Apparatus Signal Condition Monitors Provided__	52

SECTION I

INTRODUCTORY SUMMARY AND CONCLUSIONS

One of the most interesting yet perplexing aspects of elastohydrodynamic lubrication is the frictional force developed in shearing a lubricant film in loaded contacts. Most of the experimental data to date have been obtained from two disk machines in which the friction forces are measured by sliding one disk over the other. Although these data are far from complete, they show a consistent trend of how the frictional force initially increases with the sliding speed, and beyond this point an increase in sliding speed would cause a decrease in friction. The level of this friction curve is a function of the load, rolling speed, the lubricant inlet temperature, and the rheological properties of the lubricant.

Many different rheological models have been proposed to explain the observed traction curve (see Reference 1-32) but, without exception, precise prediction of traction behavior requires measurement of actual contact behavior. Hence, this state of affairs emphasizes the importance of high performance traction devices for measurement of traction behavior.

The objective of this contract was to design, develop, and fabricate a lubricant traction rig which could utilize a relatively small amount of traction test fluid. In addition, the test rig will be used to conduct research on a candidate test fluid. The pertinent design features are shown in Figure 1.

In general, the rig has been designed around the use of two crowned disks of the impinging parallel spin axis design, as shown schematically in Figure 2. The technical design requirements of the test rig were as follows:

- Test lubricant volumes as small as 250 ML
- Separation of test lubricant from support bearings
- Normal load capability up to 600 lbs.
- Test disk diameters from 1.0 inch to 1.5 inch
- Differential shaft speed accuracy better than .01%
- Variable set speeds from 2,000 to 25,000 RPM

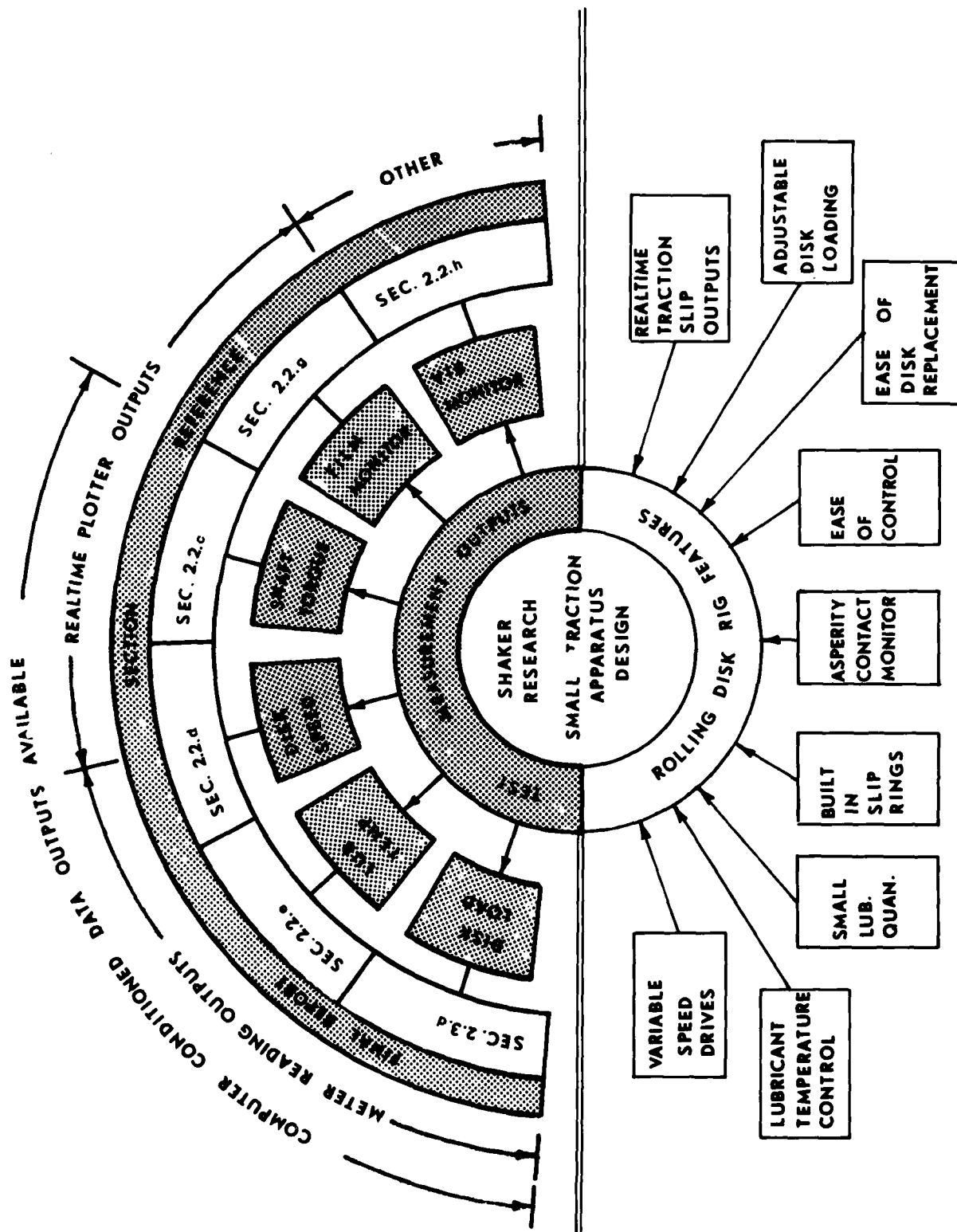
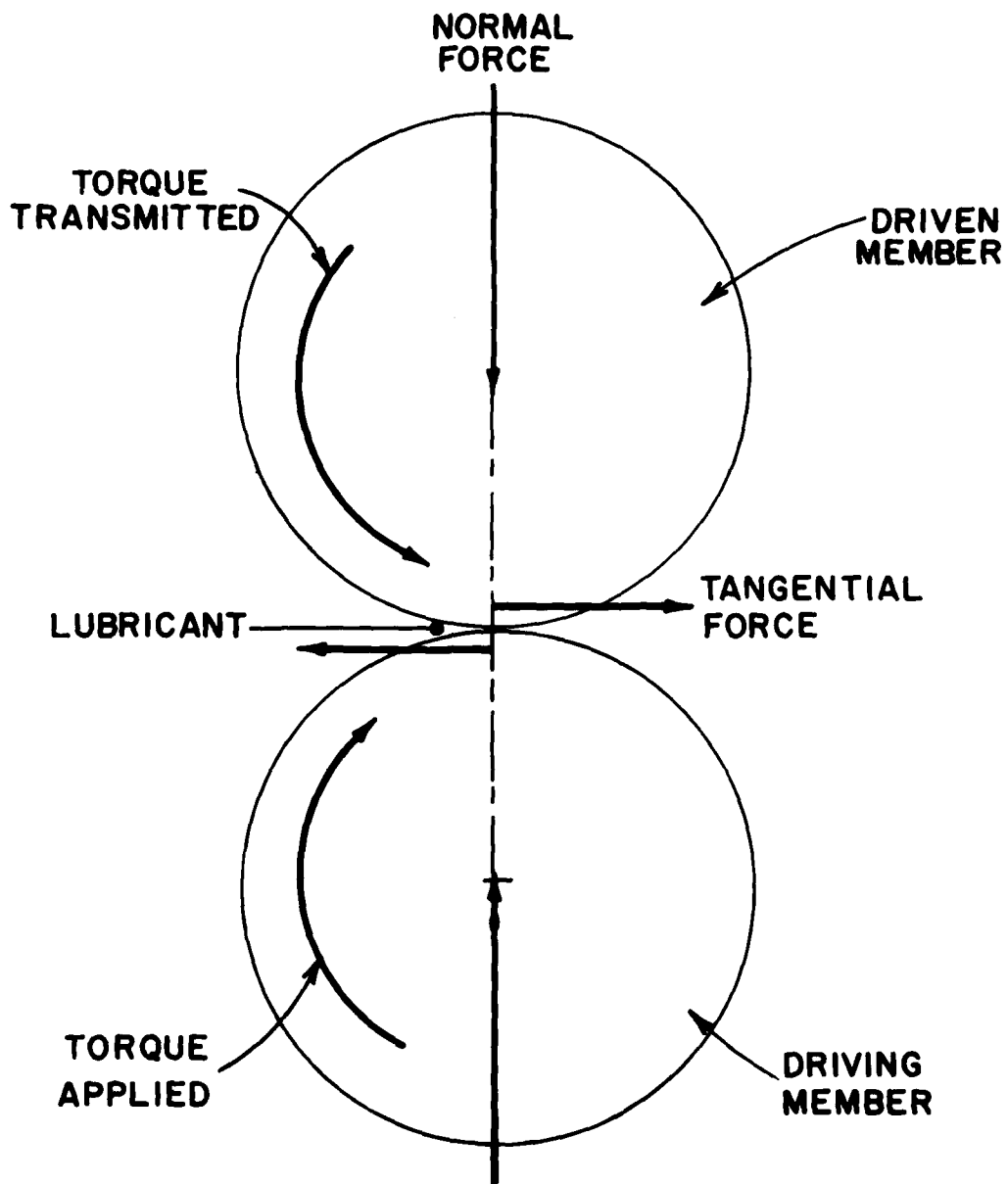


Figure 1 - Traction Rig Features



$$\text{TRACTION COEFFICIENT} = \frac{\text{TANGENTIAL FORCE}}{\text{NORMAL FORCE}}$$

Figure 2 Simple Two Disk Design for the Study of Lubricant Characteristics

- Realtime torque output with 1% accuracy
- Temperature control with $\pm 5^{\circ}\text{F}$ from 75°F to 250°F
- Electrical isolation and connection of test disks for resistive measurement output
- Incorporation of asperity contact monitor
- Computer interfacing capability of all sensing signals
- Vibration monitoring (accelerometer signals)

In addition the constructed test structure has the following features:

- An integral control panel which includes all operator controls and instrumentation readouts. The panel also has a "stand up" height bench top for use during testing.
- All mechanical components are mounted on a separate test bed arrangement approximately 24 inches off the floor for ease of set up and maintenance.
- The test disks and test lubricant supply system are located near one edge of the test bed for ease of set up.
- The test disks are easily replaceable as partial disassembly of only the test disk enclosure is required.
- The single test disk enclosure accommodates all center distance variations of different test disk diameters (from 1.0 to 1.5 inches) without modification.
- The drive system has two output shafts to permit high load, high torque capability at speeds to 10,000 RPM and moderate load, moderate torque capability at speeds to 24,000 RPM. This is provided by a simple lateral shifting of the transmission and repositioning of the high speed drive couplings.
- Provision is made for periodic retensioning of the high speed drive belt if required.
- The loading system design minimizes high speed dynamic contact forces caused by disk runout.

- Once assembled, no components will require realignment except for periods of major maintenance of the drive transmission systems.

Test Conclusions

The traction test rig was performance tested at both the Shaker Research facility and at Wright-Patterson Air Force Base during the installation period of the contract.

Appendix V contains four independent test runs for comparison purposes. Test runs in Appendix V denoted by letters "A" and "B" were taken at Shaker, while those marked with a "1" and "2" were obtained at WPAFB by Shaker personnel.

The features of the curves obtained are similar to the full traction versus slip curves obtained in Reference [2]. The peak tractive coefficient obtained from the data shown in Appendix V is approximately .03 for the 144,000 psf Hertzian contact stress loading provided by the 100 lbs. nominal disk loading. The plotted curves taken several days apart at the separate test locations provided very similar results. In fact, the curves for the 100 lb. disk loading tests can be laid one over the other and reveal identical envelopes for the 1500 RPM speed difference range plotted.

SECTION II

TECHNICAL DISCUSSION

Early measurement of the friction between gear teeth and between circular disks have placed emphasis mainly upon finding empirical correlations with the design parameters. Typical examples of contributions are by Misharin [3], and Benedict and Kelly [4]. But none of these papers were designed to promote the basic understandings of the traction between elastohydrodynamic contacts. Crook [5] must be credited with the first scientifically based introduction of a traction device.

Crook [5] used two kinds of rolling disk machines in measuring the friction in the line contact as a function of sliding speed. In the small sliding speed region he used a four disk machine which consists of a center disk surrounded by three equally spaced outer disks. Since Crook's introduction of the traction device for the study of elastohydrodynamic phenomena, there have been many contributions to the field. Some of the more important ones are summarized in Table 1.

Of particular note is the traction device developed by Smith, Walowith and McGrew [24] under Air Force Contract F33615-69-C-1305. This device permitted measurement of the total traction curve at surface speeds up to 2,400 in./sec. and at Hertz pressures approaching 400,000 psi. Traction data [1,2] for a MIL-L-7808 and 5P4E polyphenyl ether were obtained using that rig.

Although many other geometrical configurations have been suggested for traction measurements, the simple design of the two disk machine is one of the best overall choices for laboratory use. Its desirable features include:

- single point Hertzian contact for traction experimentation
- ease of test disk removal
- continuous traction curve plotting over all significant slip speeds
- separation of traction test fluid from the shafting support bearings, and
- identification and measurements of support bearing torques

TABLE 1
CONTRIBUTIONS TO ELASTOHYDRODYNAMIC LUBRICATION TECHNOLOGY

			Experimental Measurements		Interpretive Mechanisms							
			Traction	Film Thickness	Spin	Viscosity	Shear Heating	Elasticity	Non-Newtonian Flow	Structural Relaxation	Limiting Shear Stress	Other Mechanisms
1.	Smith [7]	1960	P	-	-	X	-	-	-	-	X	-
2.	Crook (III) [5]	1961	P	-	-	X	X	-	-	-	-	-
3.	Hewko, Rounds & Scott [8]	1962	P	-	X	-	-	-	-	-	-	-
4.	Smith [9]	1962	P	-	-	-	X	-	-	-	X	-
5.	Wernitz [10]	1962	P	-	X	-	-	-	-	-	-	TC
6.	Crook (IV) [6]	1963	L	X	-	X	X	X	-	-	-	-
7.	Bell, Kannel & Allen [11]	1964	P	X	-	X	X	-	X	-	-	-
8.	Fein [12]	1967	-	-	-	-	-	-	-	X	-	-
9.	Johnson & Cameron [13]	1967	L	-	-	X	X	-	-	-	X	-
10.	Dyson [14]	1970	-	-	-	X	-	X	-	X	-	-
11.	Kannel & Walowit [15]	1971	-	-	-	X	X	X	X	-	-	-
12.	Harrison & Trachman [16]	1972	-	-	-	X	-	-	-	X	X	-
13.	Trachman & Cheng [17]	1972	-	-	-	X	X	X	-	X	X	-
14.	Smith, Walowit & McGrew [1]	1972	P	-	-	-	-	-	-	-	-	-
15.	Adams & Hirst	1973	LR	-	-	X	-	-	X	X	-	PD
16.	Johnson & Roberts [18]	1974	P	-	X	X	-	X	-	-	-	RC
17.	Hirst & Moore [19]	1974	L	-	-	X	-	-	X	-	-	-
18.	Lingard [20]	1974	P	-	X	X	X	X	-	-	X	-
19.	Hirst & Moore	1975	L	X	-	X	-	X	X	-	-	PD
20.	Walowit & Smith [2]	1976	P	X	-	X	X	-	X	-	-	X
21.	Johnson & Tevaarwerk [28]	1978	P	-	X	X	-	X	X	-	-	-
22.	Bair & Winer [21]	1978	P	-	-	X	X	-	X	-	-	-
23.	Daniels [22]	1978	L	-	X	X	X	-	X	-	-	-

L = Line Contact
 LR = Line Contact in Pure Rolling
 P = Point Contact
 PD = Pressure Distribution
 RC = Roller Compliance
 TC = Integrated Given Local Traction Coefficient Over Contact
 X = Included
 - = Excluded

1. Traction Measurement

Traction measurement requires the determination of the ratio of the tangential and normal forces between two disks. The traction character of a lubricated contact changes drastically as the relative surface speeds are varied in a lubricated contact point as shown in Figure 3.

The amount of slip required to reach the point of peak tractive force depends upon many things. In general, the amount of slip required before the tractive forces begin to decrease can be stated in terms of the running speed of the disks. The peak point of sliding for most fluids is smaller than 10% of the running speed. The peak point for some fluids, however, can be as small as 1.6% of the running speed (See Reference 1). These small slips create difficult speed measuring problems.

Once the peak is reached, the tractive force begins to decrease with increasing slip speed as a result of shear heat generated in the contact zone. This decrease in tractive force with increased slip can cause drive instabilities similar to a "stick-slip" type action if care is not taken in the design of the test apparatus. The drive system must be capable of stable speed control even when the traction plot has this "negative slope" character.

Figure 4 is a display of a traction curve obtained from a test of a traction fluid. The plot contains several features of the typical traction measuring device. First of all the peak tractive force increases, of course, with contact load. In general, this number can be stated as a fraction of the applied disk loading. For most fluids this peak tractive force is less than one tenth the normal load applied between disks. This basic character of most fluids sets the design level of the rig torque measuring system. It also provides an estimate of the maximum power dissipation that will occur as a result of contact sliding.

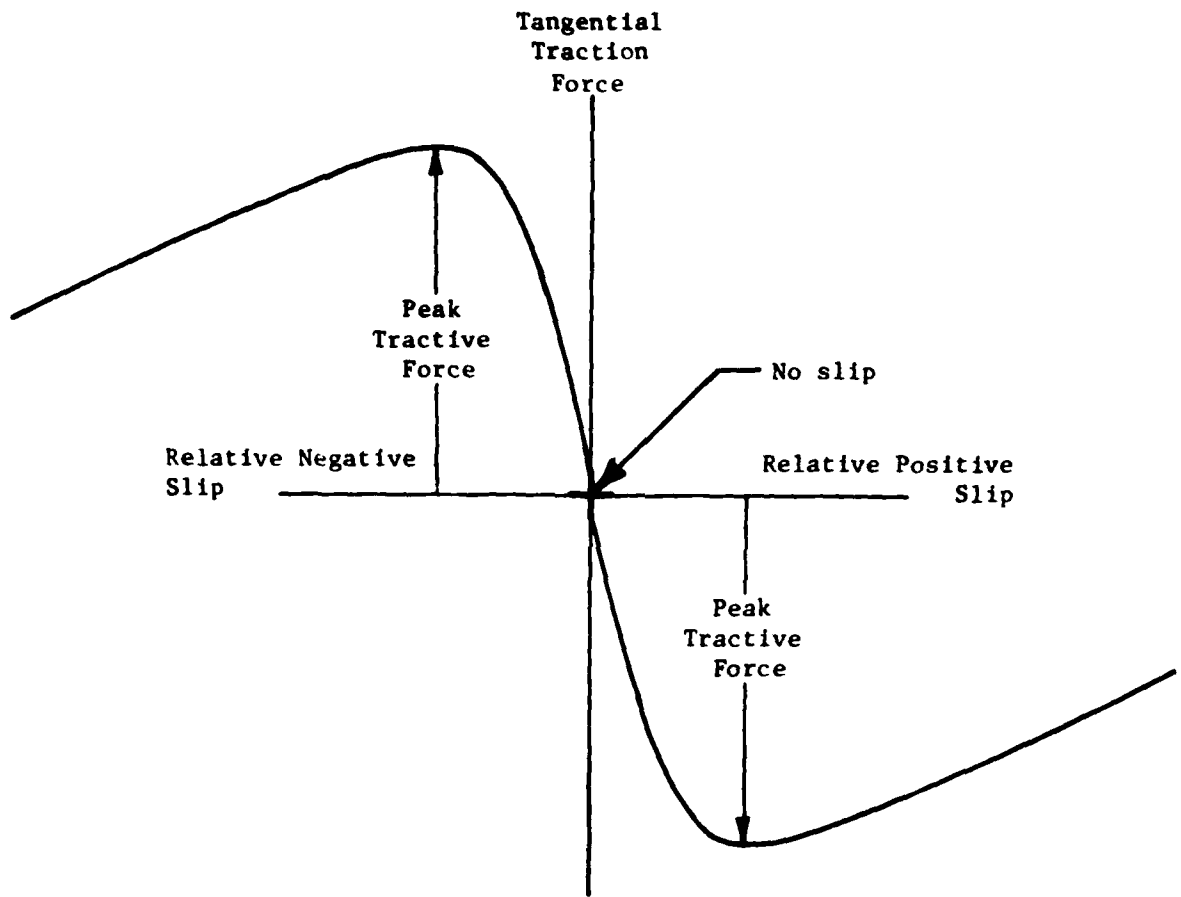


Figure 3. Tractive Forces in a Lubricated Contact as a Function of Contact Surface Sliding Speeds

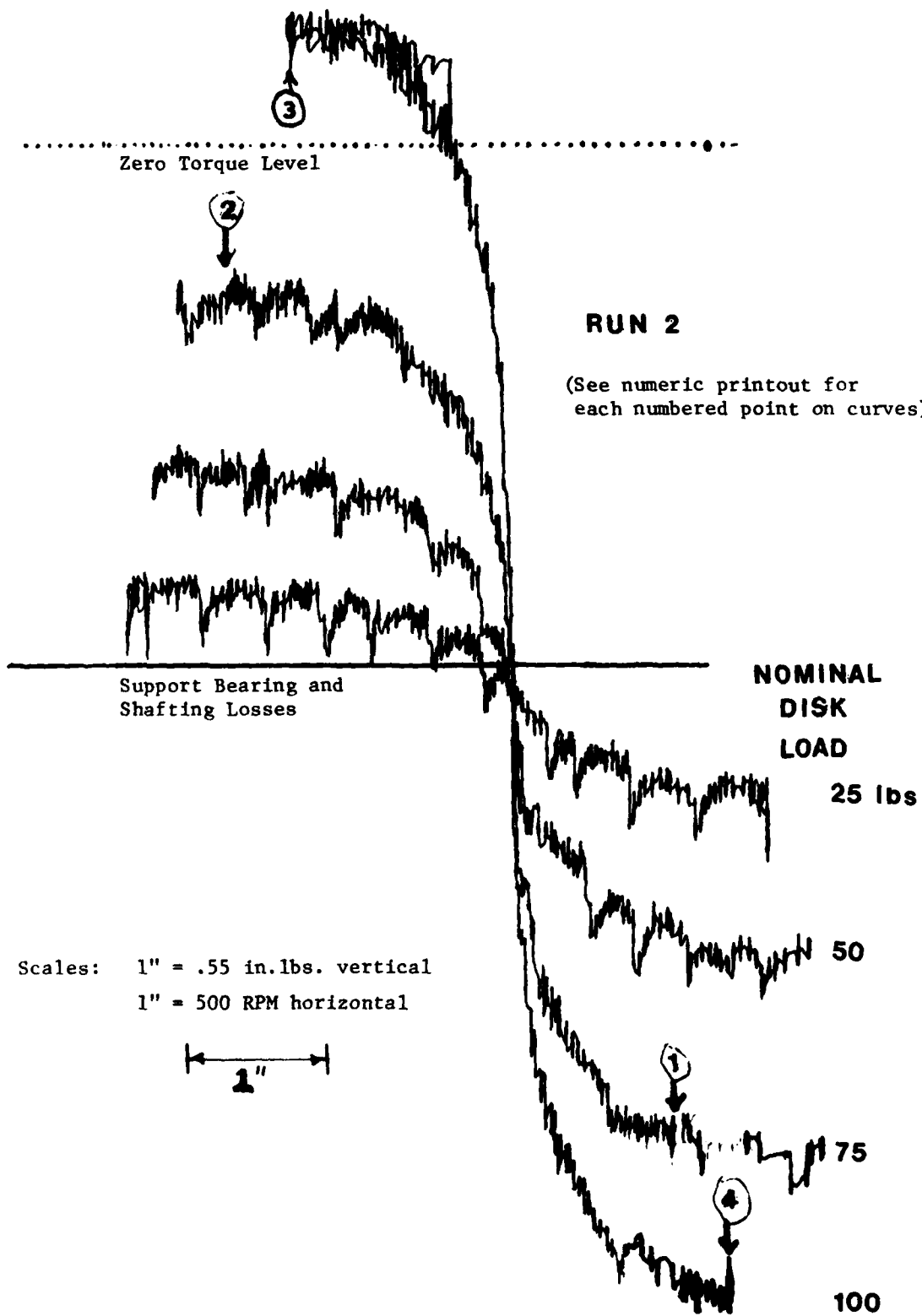


Figure 4 Traction Data From Rolling Disk Rig
With Four Separate Normal Loads

Note also from Figure 4 that there is an offset bias torque from the support bearings of the traction measuring system. This is a result of placing the torque meter outside the bearings which take up the normal disk reaction loads. The measurement of tractions in this disk apparatus provided for the measurement and display of the support bearing losses. Since the full positive and negative portions of the slip speed curve was plotted, the support bearing losses can be obtained. Measurements of traction which do not provide for determination of inherent support bearing losses must be viewed critically if accurate data on traction is desired.

The most desirable approach to traction measurement is typified by the display of Figure 4. The system used in producing that display provided for

- continuous tractive force measurements for all practical slip speeds
- output knowledge of the support bearing losses
- easy and rapid load changes, and
- temperature control of the test fluid

Systems of non-continuous (point-by-point) traction measurement are often time-consuming and susceptible to long term variation in test parameters that affect the accuracy of the results.

The tractive character of a fluid is not simply a result of commonly measurable fluid properties such as viscosity, temperature, and pressure. This fact is dramatically revealed in the traction curve of Figure 5. This plot reveals two completely different levels of tractive force that can be transferred across two different fluids which have identical ambient viscosities. The test temperatures of these two fluids were picked to match their viscosities at ambient pressure.

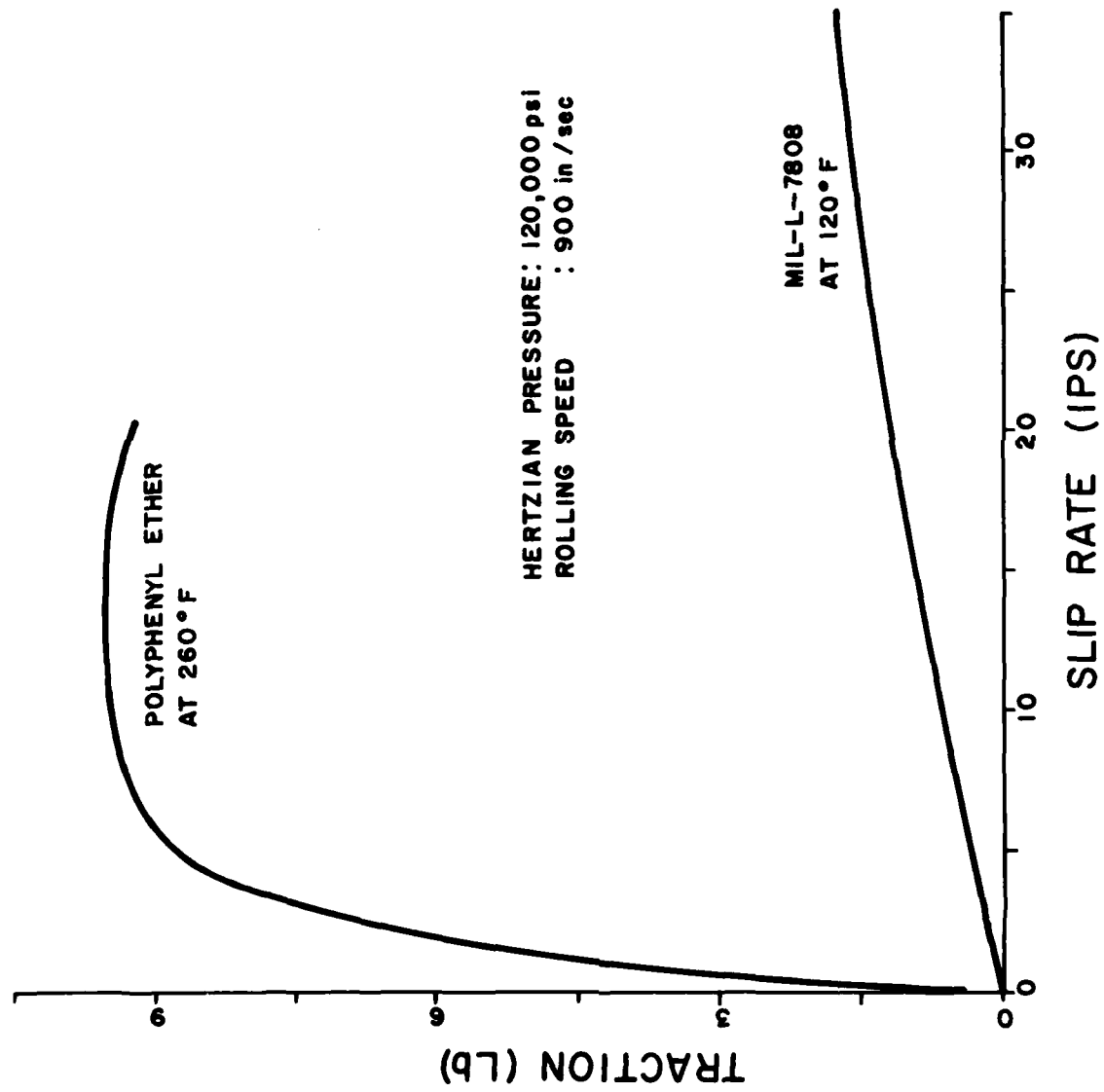


Figure 5 Difference Between Traction Curves of Polyphenyl Ether and MIL-L-7808

The answer to this perplexing situation may be in the exact character of the high pressure temperature dependence of the fluid, their non-Newtonian characteristics, or short-time dependence effects that may show up in high speed small lubricated contacts. In any case, future measurements of traction properties of fluids may reveal the subtleties of traction phenomena.

2. State-of-the-Art Traction Rig Design

The following subsections address several pertinent requirements of the traction system developed.

Some difficulties in determining traction fluid characteristics can be grouped under headings such as:

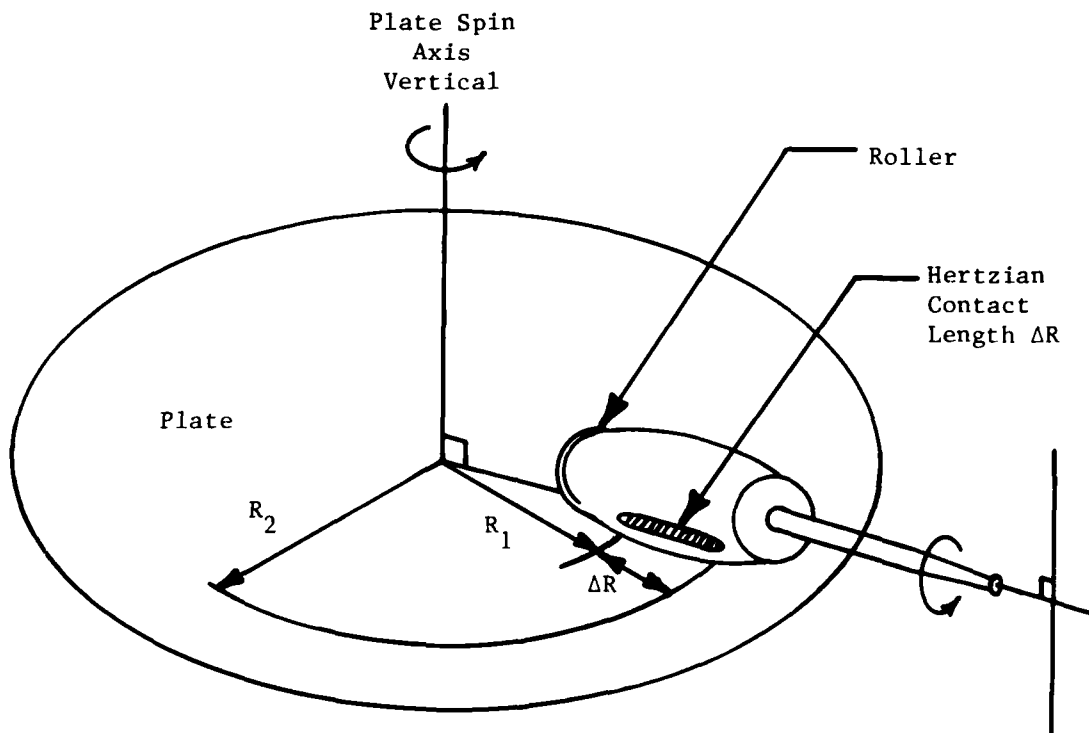
- Disk Geometric Configurations
- Disk Internal Loading Due to Runout
- Output Data Accuracies, and
- Drive Systems Considerations.

The requirements of these categories are discussed in detail in subsections below.

a. Test Disk Geometric Considerations

Basic geometric design considerations are very important in designing a traction apparatus. Hertzian contacts in traction test rigs may have a variety of sizes and special orientations. Designs with inherent skew and spin contain various amounts of slip within the loaded contact and may obscure the desired output measurement of the tractive forces. An example of such a system is shown in Figure 6.

Since the inner edge of the contact zone of the apparatus of Figure 6 will run at a different speed than the outer edge,



R_1 = Running radius of contact inner edge

R_2 = Running radius of contact zone outer edge

where $\Delta R \approx .01 \times R$, or greater

Figure 6. Traction Apparatus with Undesirable Hertzian Contact Zone Arrangement

there will inherently be different amounts of slip at every speed across the contact zone. If the ratio $\Delta R/R$ for the chosen design is 1% or more (as it is in a typical arrangement of this sort) then the tractive forces will vary across the length of the contact zone itself. Furthermore, if the center of the contact zone were to be in pure rolling one end would have positive slip while the other would have negative slip and the measured output of the tractive forces would be some combination of the two extremes.

The design concept of Figure 6 in the present development was thus avoided since basic traction forces from a test lubricant would not be obtainable in such a design. There are many others which could result in traction measurement difficulties from a basically geometric standpoint. In general, those concepts with non-parallel spinning shafts should be reviewed carefully for inherent Hertzian contact spin or skewing which could limit the reliability of the tractive measurements that could be made with them. Devices with skew or spin will normally display smaller traction coefficients than would actually be obtained with the same fluid in a system without spin or skewing.

b. Test Disk Inertial Considerations

An accurate determination of a lubricant's traction characteristics depends upon a precise knowledge of the contact load. In some traction test rig designs, built-in cyclic load variations can occur due to inherent disk inertias and run out variations in disk roundness.

Consider two massive disks, one of which is out-of-round and the pair is to be used for traction measurement. If the rotational speeds of the two disks are high enough, then the normal load between disks can be expected to change. In the case of an "egg shaped" specimen

there would typically be a dynamic twice-per-revolution loading (unloading) since at high speeds the rotational centers of the disks might not be able to follow the geometric runout. At 20,000 RPM a radial runout of about 200 microinch could be expected to impart about a "1g" acceleration to the disk system. This could represent a cyclic variation in load equal to the weight of a disk set simply loaded by gravity.

It should also be noted that since the load cells and/or reaction sensors are normally viewing the test rig lubricated contacts through relatively large inertial masses themselves that this cycle variation in loading may not show up in the typical sensing device. Some "average load" (or force) in this case would be read by the sensor even though the cyclic variations in the loading were large.

c. Torque Sensing

The two disk traction rig lends itself to the measurement of traction forces in one of two ways. Either with a torque meter on one of the shafts or with a force cell that measures the lateral forces on the shaft assembly which are perpendicular to the normal applied loads on the disks.

Although either method could be made to work, the torque metering approach is seen as the most acceptable. Among the reasons for this selection were:

- avoidance of drive belt side loads or moments
- avoidance of critical alignment tolerance to maintain contact at the peak of the disk crowns, and
- decoupling of the normal loading vector from the lateral reaction plane

The technique of measuring tractions through torque sensing is also a proven scheme for the operating conditions required. Table 2 displays the available accuracies of commercially available torque sensors that can operate at maximum speeds of 25,000 RPM.

The maximum design load required was 600 lbs and a typical peak traction coefficient of .07 yields a tangential force of about 42 lbs. A maximum disk design radius of .75 inches therefore requires a torque sensor with at least 31 in-lbs. of measuring capability. The torque resolution (or lowest torque output) of these torque sensors is typically one thousandth of the full scale of the instrument. The selection for this application was therefore a 100 in-lb. full scale capacity instrument.

d. Rolling and Slip Speeds

Although precise absolute disk speed measurement of a traction measuring apparatus was required, the most critical speed requirement was in the slip speed determination. A measurement accuracy of .01% or better of the slip speed measurement was required.

This high accuracy of slip speed determination was justified in light of the types of traction slip curves one encounters in practice.

In particular, test fluids such as polyphenyl ethers have full peak traction points near 1% of the base rolling speed for high loads. For this reason the latest electronic techniques of measuring shaft speeds were used in the slip speed measurement design.

Measurement of the slip speeds between the two primary shafts of the traction rig makes use of digital electronics. Each shaft contains a once-per-revolution reference pulse output detector (see

TABLE 2

COMPARISON OF THREE TYPES OF
ROTATING SHAFT TORQUE SENSORS

	STRAIN GAGE TYPE		TVDT MAGNETIC TYPE
	With Slip Rings	Transformer	
Non-linearity	0.1 % F. S.	0.1 % F. S.	2.0 % F. S.
Readability	.06% F. S.	.06% F. S.	.06% F. S.
Effect of temperature on output/50°F change	0.1 % Rdg.	0.1 % Rdg.	0.1 % Rdg.
Effect of temperature on zero/50°F change	0.1 % F. S.	0.1 % F. S.	0.1 % F. S.
Effect of differential temperature change	Negligible	Negligible	2.0 % Rdg.
Field Service	Routine Cleaning	None	None

F. S. = Full Scale
Rdg. = Reading

Figure 7. These two output pulses are used under program control to clock the rotational period spanned for ten revolutions of each shaft separately. Once timed, the period is mathematically inverted to represent the rotational frequency of each shaft. The two frequencies are again manipulated through a preprogrammed processor to obtain their difference and thus, the operating slip speed of the disks.

At 2,000 RPM the maximum cycle time is about 0.6 seconds. At 24,000 RPM the updated speed difference is determined approximately every .05 seconds.

In addition, the rolling speed of the traction apparatus is monitored to about 1-2% of the actual running speed. Since traction forces are not highly influenced by small variations in running speed, this accuracy is sufficient.

2.2.5 Lubricant Temperature

Tractive forces in a lubricated contact are influenced by the temperature of the fluid at the inlet zone to the contact as well as within the contact. Figure 8 is a display of the traction variations one can get with a Mil-L-7808 oil by changing the temperature of the fluid feeding the contact.

The temperature of the fluid at the inlet sets the film thickness of the Hertzian contact through the viscosity of the fluid at the ambient inlet pressure. As the temperature rises, the fluid viscosity drops yielding a thinner contact film if all other conditions are fixed. Figure 8 shows that the lowest viscosity transmits the lowest tractive force as well.

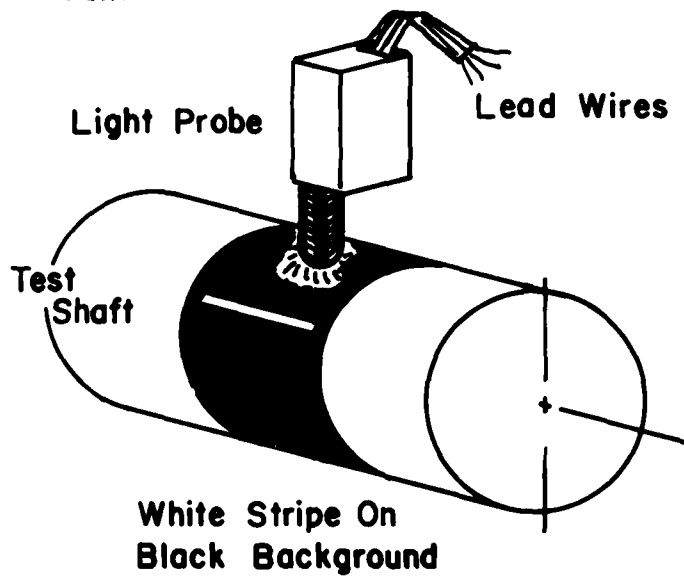
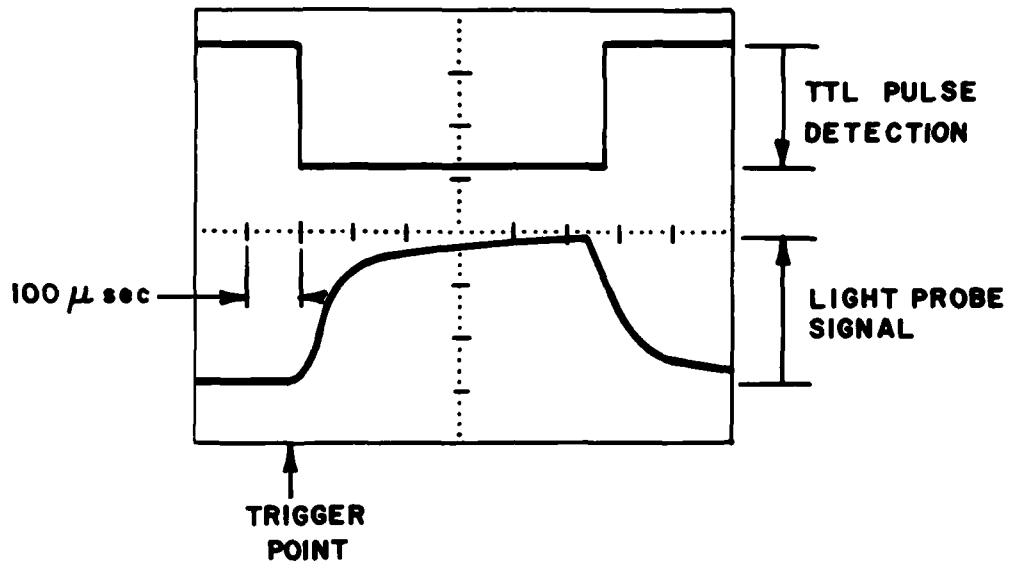


Figure 7 Sample Shaft Speed Timing Signal Output and Detection

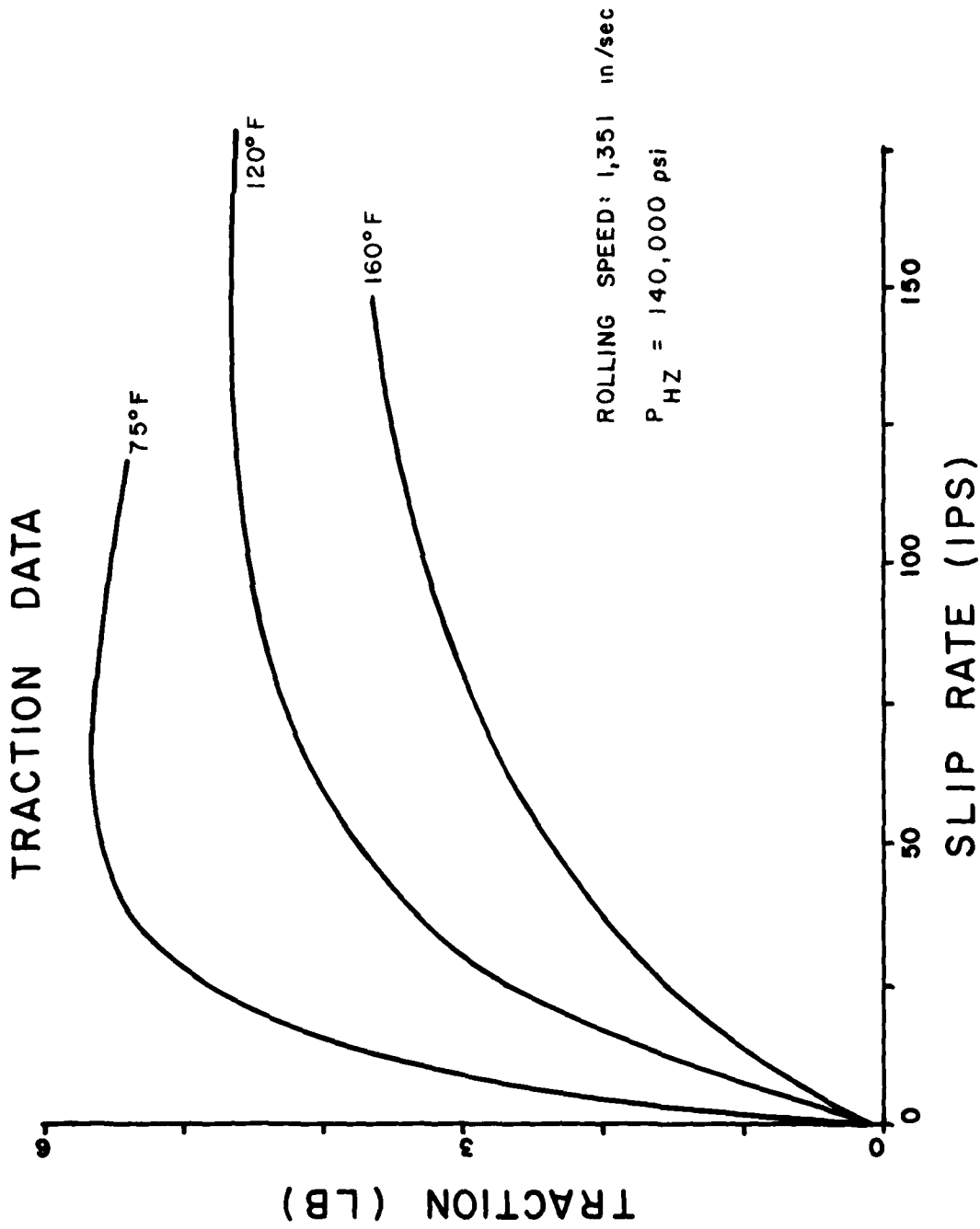


Figure 8 Affect of Lubricant Inlet Temperature on Traction Characteristic

The sensitivity of the traction curve to changes in bulk lubricant temperature are not very large as shown. In going from 75°F to 160°F the viscosity of the fluid has changed by more than a factor of ten, but the tractive forces at every slip speed have roughly a 2 to 1 ratio. For this reason the bulk temperature of the test fluid need only be monitored to about a 5°F accuracy over the 75°F to 250°F range of operating temperatures. Standard commercially available thermocouple sensing and digital readout displays used in the present design offer 1°F or better of temperature sensing.

Although the temperature of test fluid bath can be measured accurately enough, it must also be maintained at a preselected level during testing. Shear heating in the contact load zone must be dissipated at the rate it is generated or the test fluid will heat up. The power generated in the single point contact of the crowned test disk can be written in horsepower as

$$\text{POWER} = \frac{\text{SF} * \text{NORMAL LOAD} * \text{TRACTION COEFFICIENT} * \text{DISK RADIUS}}{63,024}$$

where SF represents the slip frequency of the test disk shafts in revolutions per minute. An estimate of power generated for typical values of traction is

$$\text{POWER} = \frac{(2,400) (600 \text{ lbs.}) (.07) (.75)}{63,024} = 1.19 \text{ HP}$$

where the maximum loads, speeds, and shaft diameters for this design have been assumed. This level of power generation within the contact load would occur only if the typical peak traction coefficient of approximately .07 were continuously present.

The power generated within the contact zone during testing is dissipated either through the test disks or through the test lubricant. If one

assumes that all the heat generated as calculated above is transferred to the test lubricant then the circulating lubricant reservoir must carry away from 1 to 2 horsepower. If this is not done then constant test fluid temperatures in the circulating sump are not maintained. The traction disks are jet fed in order to maintain sufficient and proper feeding, thus it was possible to pass the pumped fluid through a small heat exchanger. For design purposes, it was assumed that the 250 ml design volume of test fluid is circulated through a constant temperature bath. This bath is able to remove heat from the circulating test fluid up to the expected 1 to 2 horsepower level as required.

f. Lubricated Contact Loading

Traction forces are directly proportional to the applied normal load in the low slip portion of the traction curve. For this reason, accuracy of the normal load applied will affect the accuracy of the traction coefficients determined for the test fluid.

Inspection of the Hertzian stress levels of Table 3 gives a typical resolution accuracy required. In general, it was assumed that a certain Hertzian stress level was to be set for any one given traction curve plot. From Table 3 then, a 5 lb. variation in normal loading at a 95 lb. load level will result in an accuracy of about 2% in the resulting 141,741 psi stress level. The stress level accuracy changes for each disk geometry and load level but this example illustrates the typical range achievable.

The result of this discussion is that a commercially available load cell with a .1% full scale readability was sufficient for measuring and setting test loads up to 600 lbs.

TABLE 3

HERTZIAN STRESSES FOR VARIOUS DISK NORMAL LOADS (HEAVY LOADS)

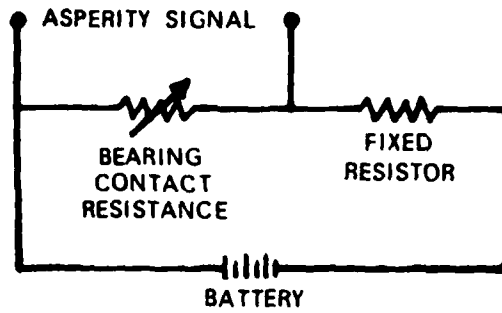
HERTZ STRESS	CONTACT RADIUS A	ELLIPSE RADIUS B	#-----BODY RADII-----#				LOAD ON CONTACT
			ROLL		CROWN		
PSI	MILS	MILS	#1	#2	#1	#2	LBS
			IN	IN	IN	IN	
53118	24.9	1.8	.5625	.5625	35	35	5
66924	31.3	2.2	.5625	.5625	35	35	10
76609	35.9	2.6	.5625	.5625	35	35	15
84319	39.5	2.8	.5625	.5625	35	35	20
90830	42.6	3.0	.5625	.5625	35	35	25
96522	45.2	3.2	.5625	.5625	35	35	30
101611	47.6	3.4	.5625	.5625	35	35	35
106236	49.8	3.6	.5625	.5625	35	35	40
110490	51.8	3.7	.5625	.5625	35	35	45
114439	53.6	3.8	.5625	.5625	35	35	50
118134	55.4	4.0	.5625	.5625	35	35	55
121610	57.0	4.1	.5625	.5625	35	35	60
124898	58.5	4.2	.5625	.5625	35	35	65
128022	60.0	4.3	.5625	.5625	35	35	70
131001	61.4	4.4	.5625	.5625	35	35	75
133849	62.7	4.5	.5625	.5625	35	35	80
136582	64.0	4.6	.5625	.5625	35	35	85
139209	65.3	4.7	.5625	.5625	35	35	90
141741	66.4	4.8	.5625	.5625	35	35	95
144185	67.6	4.8	.5625	.5625	35	35	100
153219	71.8	5.2	.5625	.5625	35	35	120
161298	75.6	5.4	.5625	.5625	35	35	140
168640	79.1	5.7	.5625	.5625	35	35	160
175392	82.2	5.9	.5625	.5625	35	35	180
181662	85.2	6.1	.5625	.5625	35	35	200
187526	87.9	6.3	.5625	.5625	35	35	220
193044	90.5	6.5	.5625	.5625	35	35	240
198264	93.0	6.7	.5625	.5625	35	35	260
203223	95.3	6.8	.5625	.5625	35	35	280
207951	97.5	7.0	.5625	.5625	35	35	300
212473	99.6	7.2	.5625	.5625	35	35	320
216810	101.7	7.3	.5625	.5625	35	35	340
220981	103.6	7.5	.5625	.5625	35	35	360
225000	105.5	7.6	.5625	.5625	35	35	380
228880	107.3	7.7	.5625	.5625	35	35	400
232632	109.1	7.8	.5625	.5625	35	35	420
236268	110.8	8.0	.5625	.5625	35	35	440
239795	112.4	8.1	.5625	.5625	35	35	460
243221	114.1	8.2	.5625	.5625	35	35	480
246553	115.6	8.3	.5625	.5625	35	35	500

Comments concerning the stroke of the normal loading system should also be mentioned. The loading system had to be able to follow or track the inevitable disk runout that is always present without varying the applied load. This was accomplished by using an air piston loading mechanism. Such an arrangement provided for the dynamic load following capability, as well as for each removal of the disks for maintenance. A loading cylinder with a 3 to 4 inch stroke was selected to enable the shafts to be separated laterally for ease of disassembly.

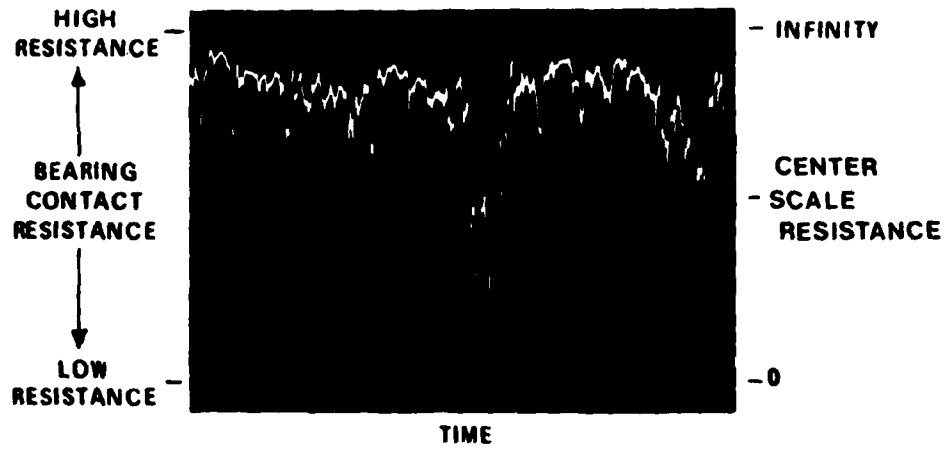
g. Film Condition Monitoring

The proposed test disk assembly design provides for contact film condition monitoring through the use of slip rings and electrical isolation of the test disks. This allows for either capacitive or electrical resistivity monitoring of the contact zone during traction investigations. Simultaneous capacitive and resistance measurements are not possible since a single set of isolation slip rings are used.

Properly-lubricated contacts operate with a minimum of metal contact between the disks. Since most lubricants are organic hydrocarbons, a high average resistance is usually maintained between disks. Fluctuations in contact resistance during operation provide asperity signals which are detected in the present design with electrical circuitry as shown in Figure 9(a). A small D.C. voltage applied across the disks during the detection cycle provides the actual asperity signal. The signal output from a contact with some asperity interaction is shown in Figure 9(b). A time average output of the percent of contact for a lubricated metal contact is displayed in Figure 10. The three curves show the basic resistance output dependence with various loads and speeds of operation of a typical lubricated contact.



(a) Electrical Contact Diagram



(b) Contact Resistance Signal

Figure 9

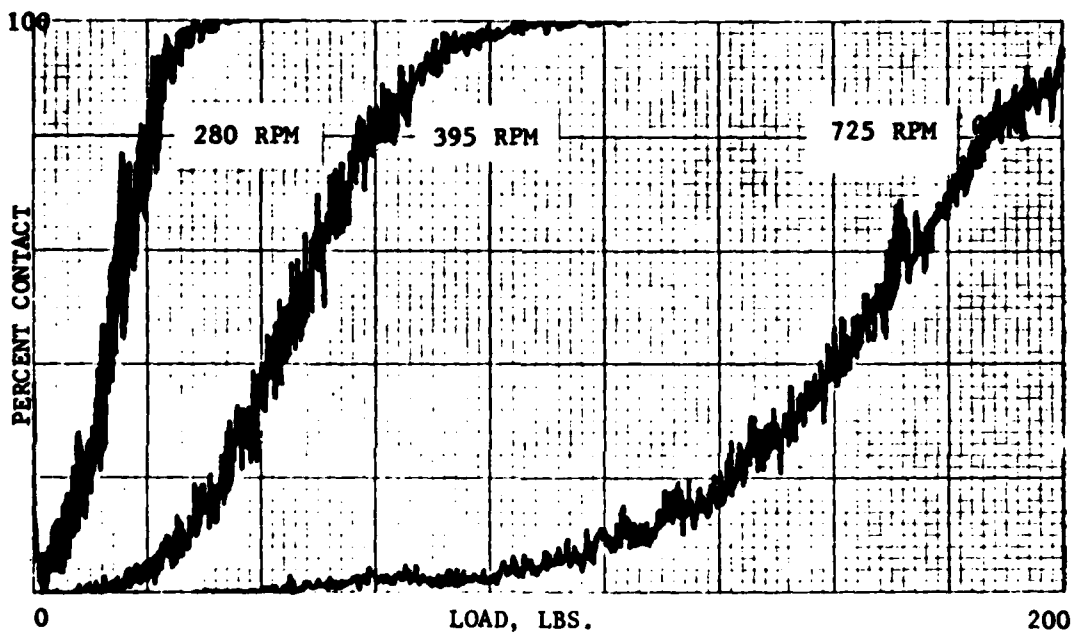


Figure 10 Asperity Contact Load/Level Sensitivity

The designed traction system incorporates an electrical contact monitor in the equipment supplied. Capacitive monitoring of the loaded Hertzian contact zone is also possible with the designed rig, although capacitive measurements of the traction fluid were not carried out in the study.

h. Vibration Detection

The primary sensors used for vibration detection in the industry are displacement or accelerometer sensors. These fingertip sized devices provide high frequency output voltages proportional to displacement or acceleration. The designed traction apparatus has a pair of mounted displacement and accelerometer sensors suitable for monitoring vibration of the test assembly. The accelerometer used has a frequency response ranging from 5 to 25,000 cycles per second. The displacement probes on the other hand can respond to movements from 0 to 15,000 cycles per second.

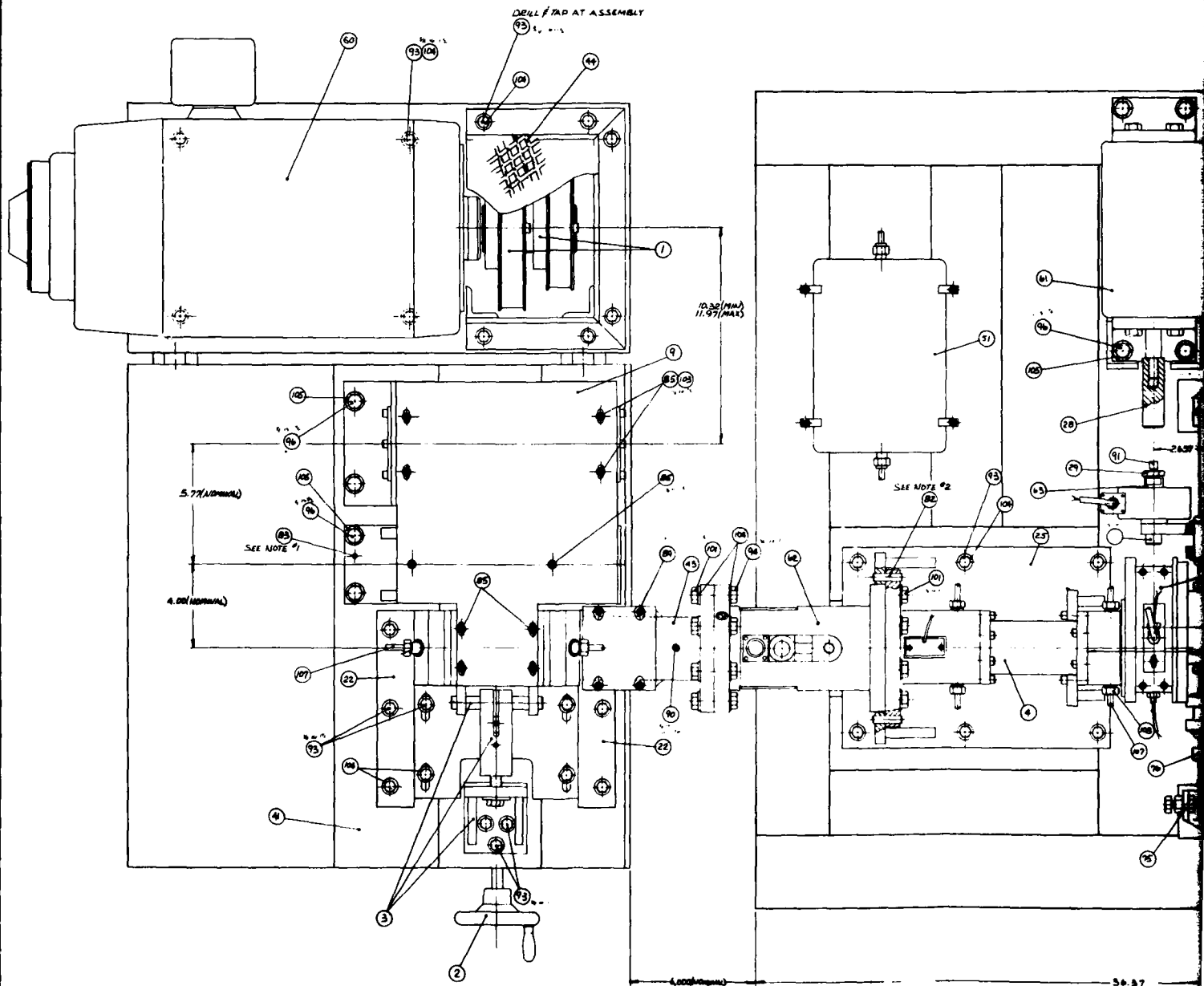
3. Description of the Design

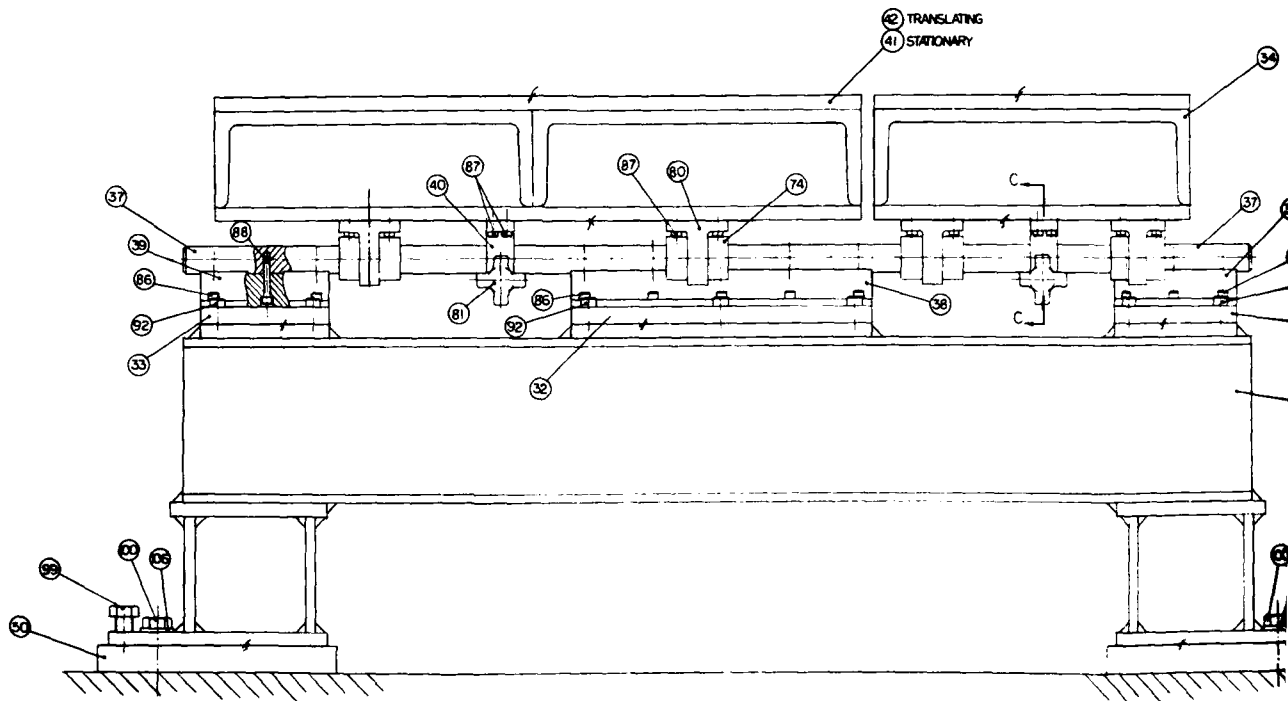
A plan and end view of portions of the designed test apparatus are shown in Figures 11 and 12. Photographs of the control panel and instrument panel are shown in Figure 13.

a. Description of Overall Arrangement

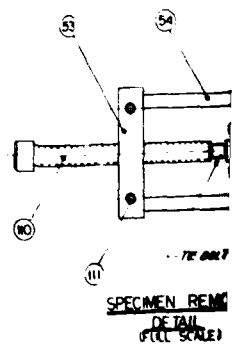
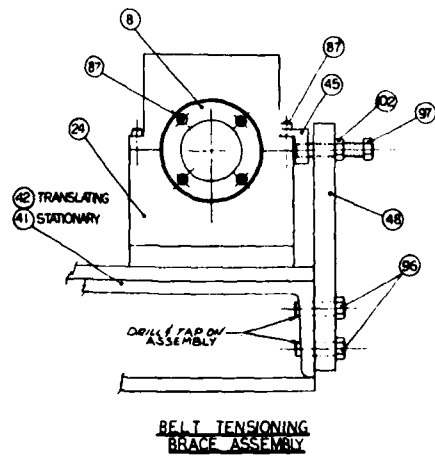
Referring to Figure 11, the basic mechanical apparatus consists of the following major subassemblies:

- a. two drive transmission with motors
- b. two test disks
- c. one loading mechanism
- d. one load sensor
- e. one torque meter





TYPICAL SIDE VIEW



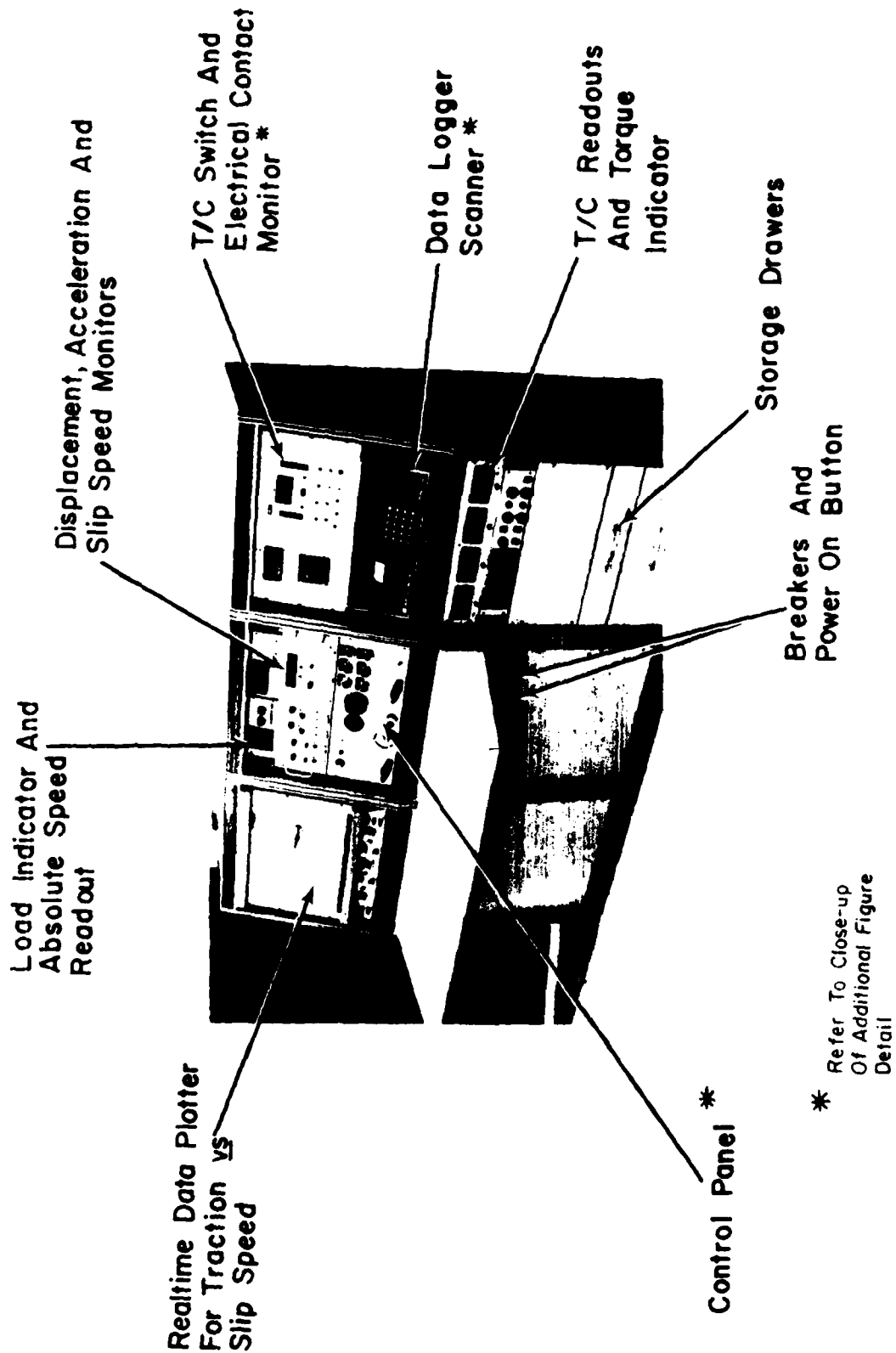


Figure 13 Drawing of Instrument and Control Panel

- f. one temperature controlled lubricant circulating system
- g. a test disk enclosure

All of the above are mounted on one of three welded base structures. The three bases are in turn mounted on a pair of steel channels for alignment and installation purposes. Figure 14 is a typical test room layout with rig dimensions shown for set-up purposes.

b. Drive System

The two transmission assemblies are mirror images of each other. A step-up transmission is required because reasonably priced commercially available variable speed drives are generally limited to speeds below 4,000 RPM. The drive transmission assemblies increase the speeds of the variable speed drives to the desired test speeds through a series of step-up belts. Two transmission output shafts are provided. Output Shaft 1 is a high torque (limited only by drive motor speed torque characteristics) moderate speed (approximately 11,000 RPM maximum) output, while transmission output Shaft 2 is a high speed (24,000 RPM maximum) moderate torque (approximately 50 in.-lb. maximum) output. Both the output shafts are at the same elevation and either can be connected to the disk support spindles through the drive couplings by moving the transmission assemblies on their mounting ways shown in Figure 12.

For the high speed (24,000 rpm) end a flat belt operating in the 10,000 to 12,000 ft./min. range was selected. This was about the optimum velocity range for a thin flat belt in that higher velocities result in excessive centrifugal stresses and lower velocities create high flexural stresses (because of small pulley diameters) and high tensile loads (for a given power transmitted.) The flat belt speed ratio selected was approximately 2.2:1 which puts the low speed shaft (output Shaft 1) at approximately 11,000 RPM. This was a reasonable speed for high quality commercially available grease lubricated pillow block bearings having shield-type seals.

TEST ROOM LAYOUT (NOT TO SCALE)

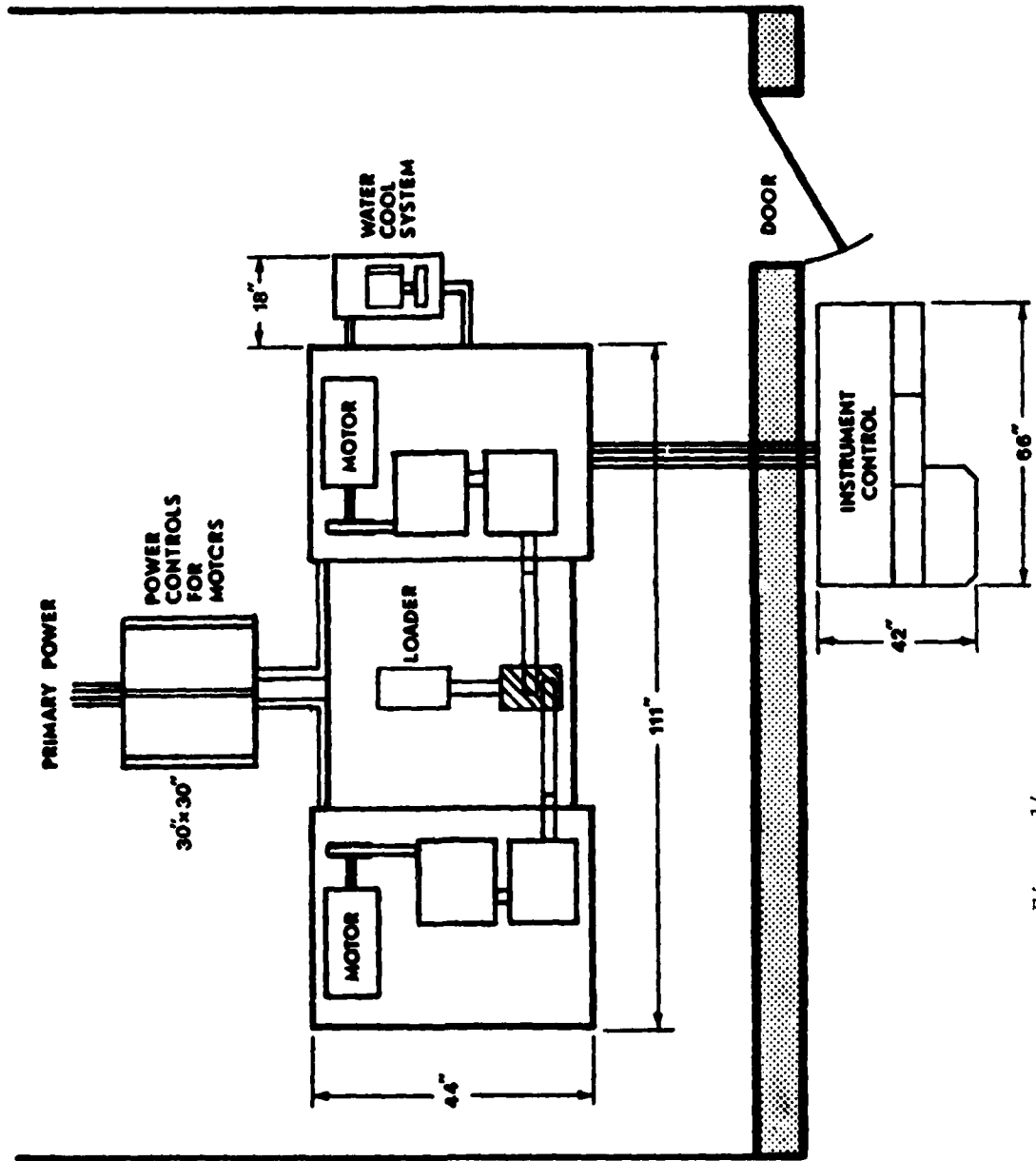


Figure 14

Except for the drive motor/brake pulley (which is discussed later), all pulleys are straddle mounted which tends to minimize support bearing loads. For the high speed shaft, a 25 mm bearing (600,000 DN at 24,000 RPM) has a computed L_{10} life in excess of 2,000 hours under the maximum belt tension (approximately 165 lb.). Under maximum speed conditions (24,000 RPM) approximately 2 HP is consumed by the six support bearings in the transmission assembly.

For the first two step-up belt combinations, standard toothed-type flat belts are used. Standard one inch wide by one-half inch pitch belts are more than adequate. All transmission pulleys were dynamically balanced to assure smooth operation at the higher speeds.

In the case of the last step-up flat belt, retensioning and replacement may be periodically required due to belt creep. To accommodate periodic flat belt maintenance and bearing replacement, the high speed bearing housing was provided with a bolt-on type set of ways which fixes its parallelism with respect to output Shaft 2. Proper belt pretensioning is achieved by pulling on the Number 2 output shaft housing through the calibrated "flat belt pretension spring." Actual pretension force was determined by calibrating the built-in spring washer sets.

The belt transmission system described in Figures 15 and 16 is inherently capable of handling power flow in either direction (into or out of the drive motor/brake) in that it contains no idlers or other components which limit the tension in either side of the belt. Furthermore, any backlash is highly friction damped making operation at the zero slip condition well controlled.

Figure 17 summarizes the transmission output torque design limits. These limits are based upon conservative belt tension (resulting from transmitted torque, pretension, and centrifugal force) design values

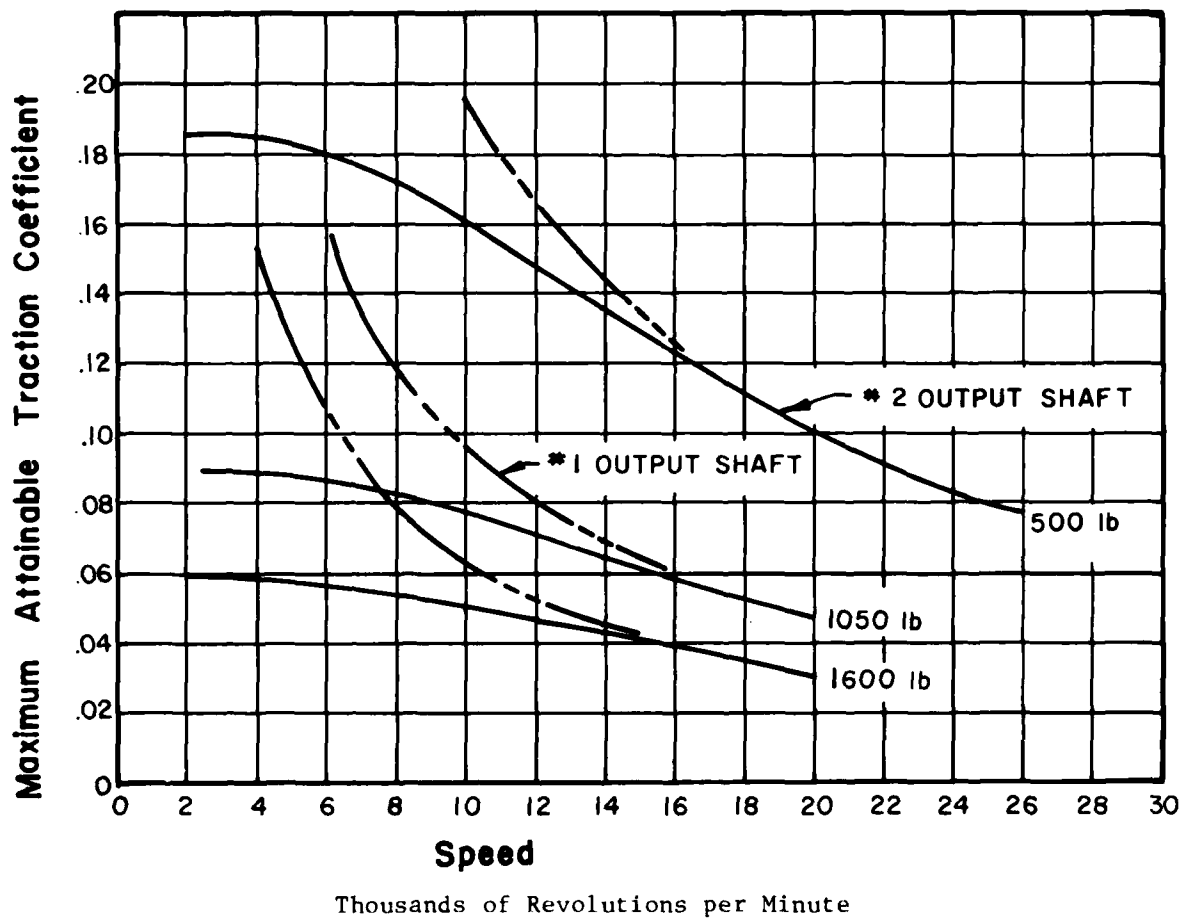
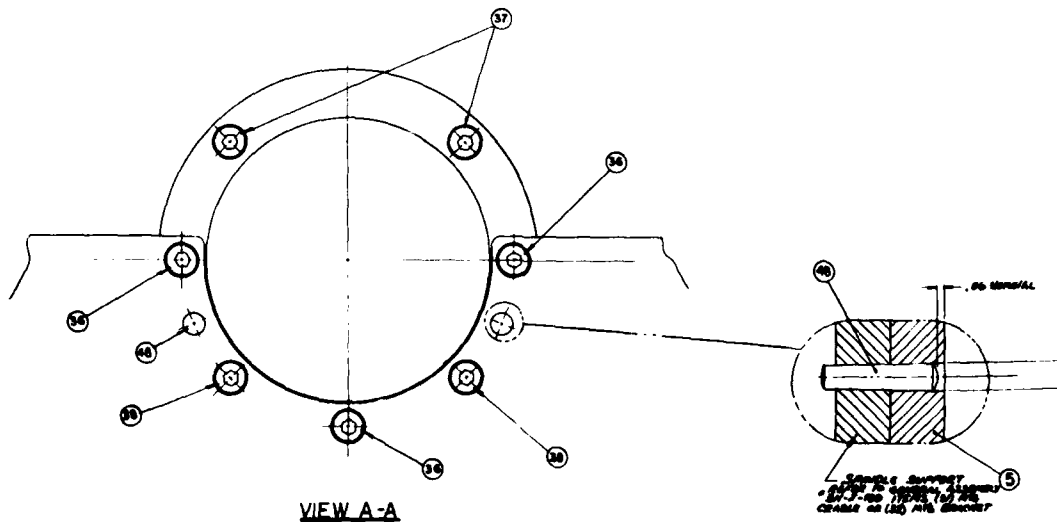
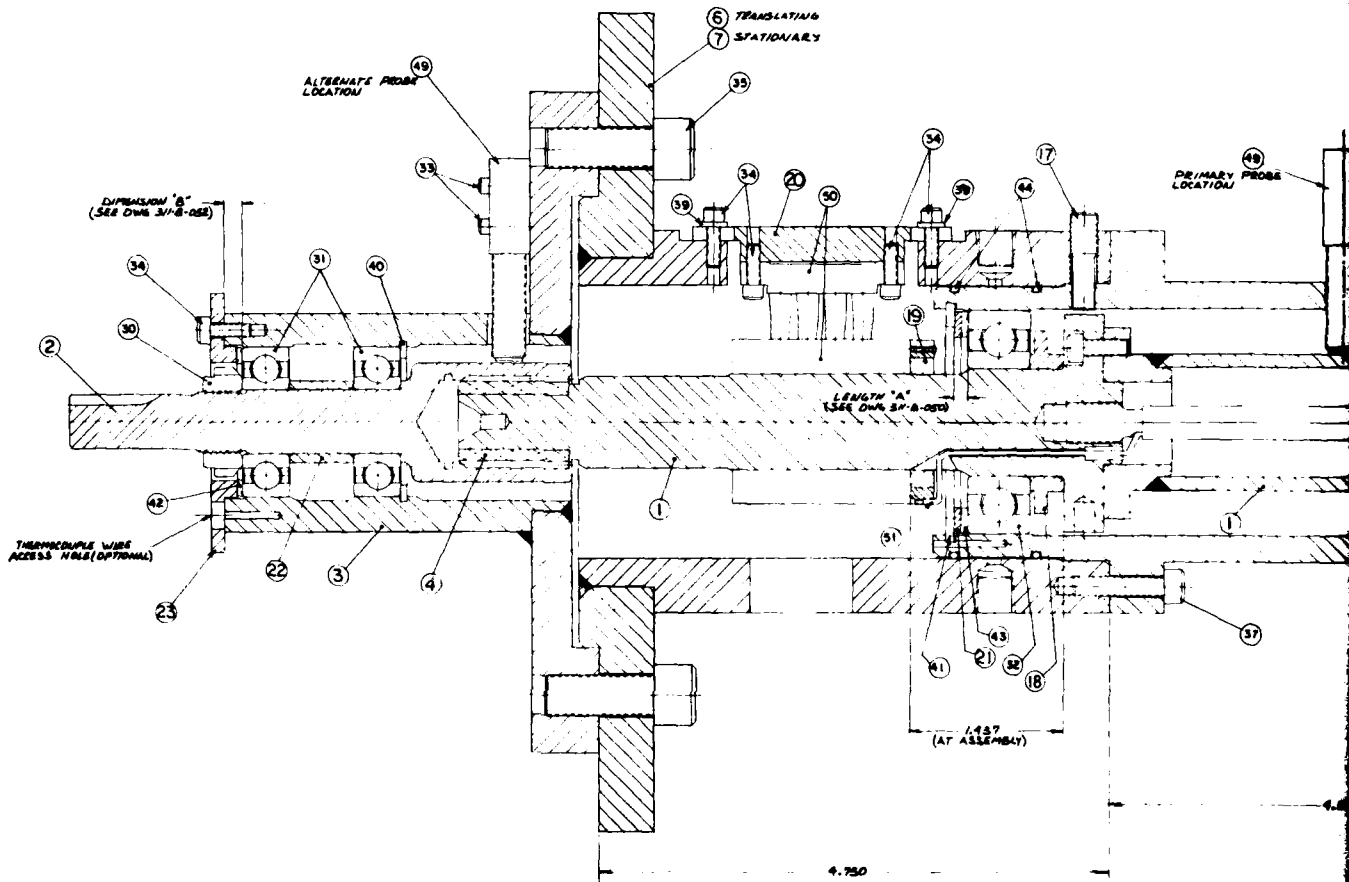
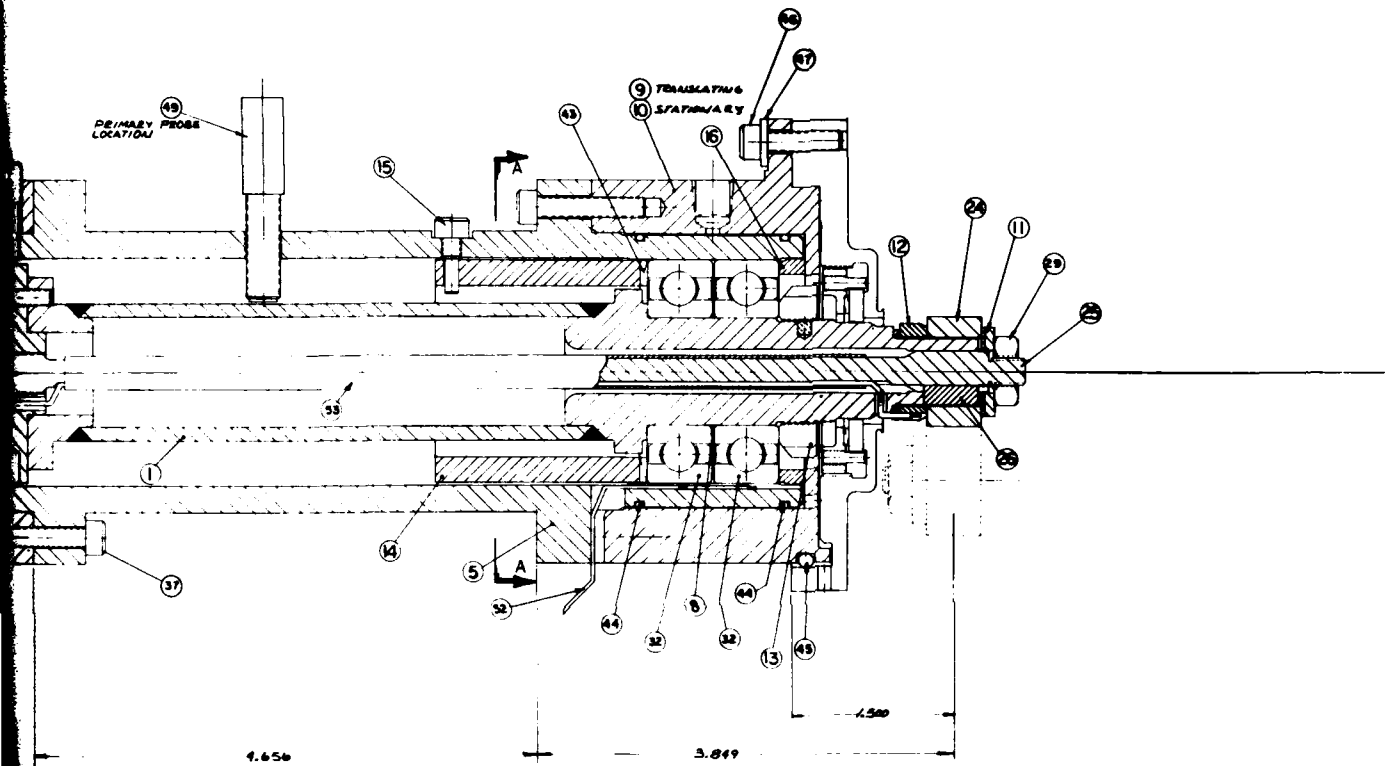


Figure 15 Maximum Attainable Traction Coefficients for 1.125 inch Diameter Test Disks





SEE CH 1
 ALL SPINDLE FLANGES AND
 SPINDLE ASSEMBLY SHALL BE SPINDLE FLANGES AND
 SPINDLE ASSEMBLY BY THIS DRAWING WITH 21.1000
 SHALL BE MADE WITH TAPER BEARING TO DIMENSIONS
 SHOWN FOR AMERICAN STANDARD TAPER ROLL

Figure 16

- ⑥ TRANSLATABLE
- ②② STATIONARY

DIMENSIONAL TOLERANCES UNLESS OTHERWISE SPECIFIED		SHAW-WORTH Research Corporation	
FRACTIONS .0005		RESEARCH CORPORATION	
DECIMALS .001		RESEARCH CORPORATION	
ANGLES .001		RESEARCH CORPORATION	
HOLE POSITION .001		RESEARCH CORPORATION	
HOLE DIA .001		RESEARCH CORPORATION	
HOLE LENGTH .001		RESEARCH CORPORATION	
HOLE TAPER .001		RESEARCH CORPORATION	
HOLE SURFACE .001		RESEARCH CORPORATION	
HOLE END .001		RESEARCH CORPORATION	
HOLE CHAMFER .001		RESEARCH CORPORATION	
HOLE ALL OTHERS .001		RESEARCH CORPORATION	
TITLE		SUPPORT SPINDLE ASSEMBLY	
SCALE		DOUBLE 3/4" = 1" - 500	
DRAWN		CHECKED	
DATE		DATE	

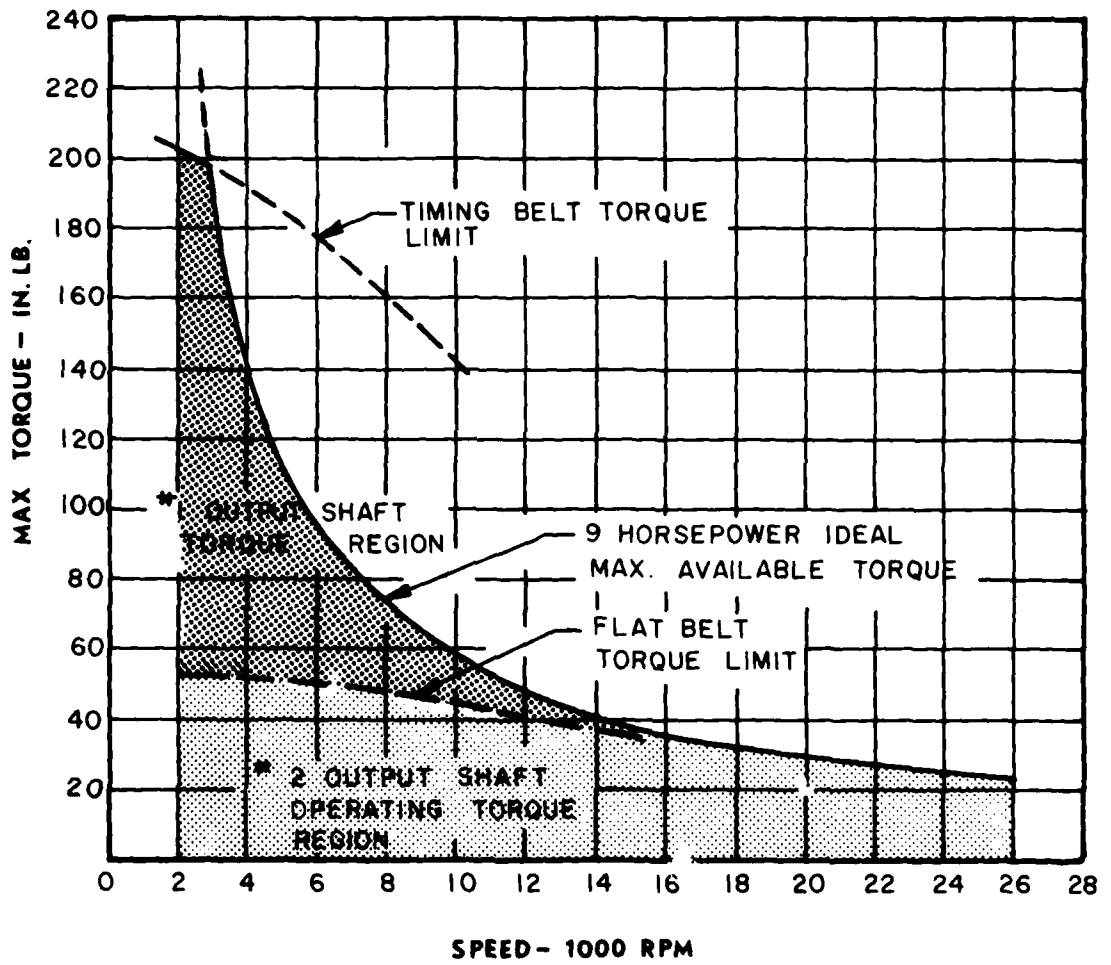


Figure 17 Drive Transmission Torque Limits

for the sizes used. Figure 17 is a design curve which shows an "ideal" constant nine horsepower speed torque characteristic which allows for an average one horsepower transmission loss over the entire speed range. The shaded areas indicate the operating torque capability of each of the output shafts. Clearly the upper end of the Number 1 output shaft torque region defined by the "ideal" motor curve will not likely be attainable because of the speed-torque characteristics of the drive motor. In the case of an SCR controlled motor, which is normally a constant torque device, this limit could only be reached by an infinitely variable transmission. However, with the pulleys shown in Figure 11, low speed torques approaching 120 in.-lbs. are readily attainable.

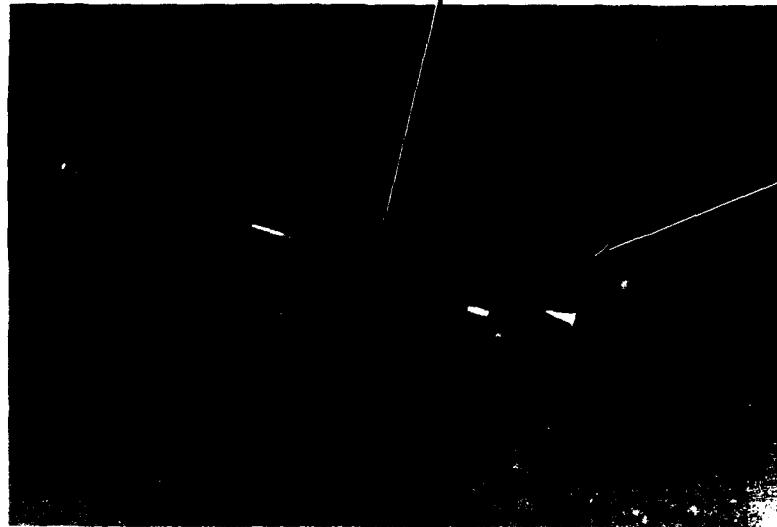
c. Test Disk Support Spindles

A cross-section drawing of the test disk support spindle is shown in Figure 16. The test disk is cantilevered from the end of the spindle and held in place by a self-locking nut. (See photos of Figure 18.) The cantilevered approach is a result of two primary factors:

- a. the desire for ease of assembly and disassembly of the test disks, and
- b. the large bearing size relative to the small test disk size required to support the design load.

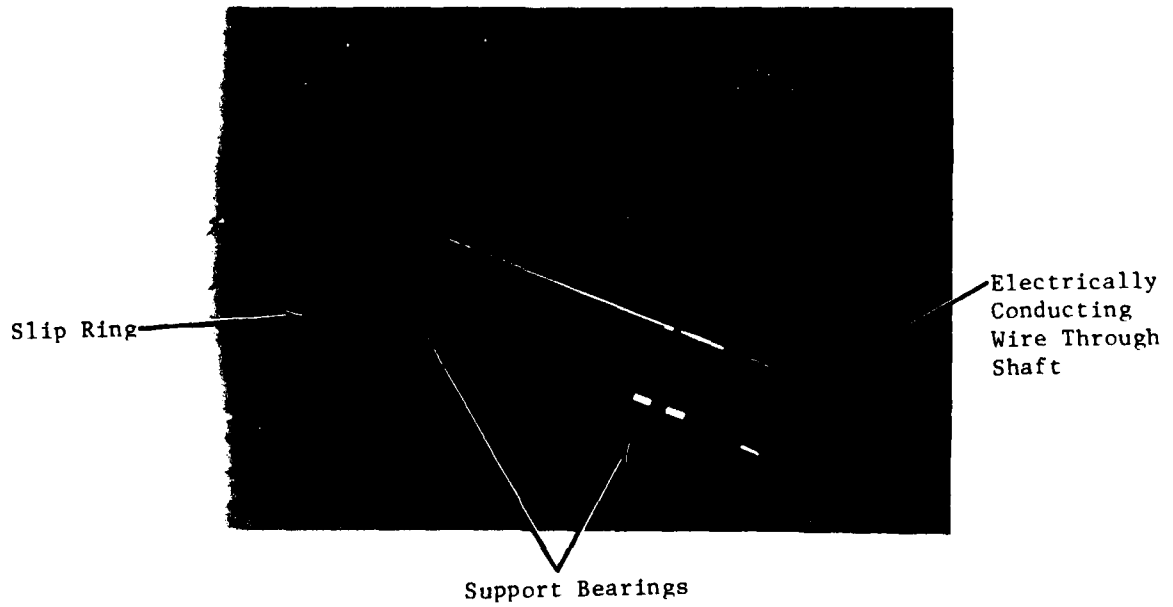
Cantilevered disks are clearly superior to straddle-mounted disks from an ease of assembly and disassembly point of view. However, from the standpoint of reaction bearing loads the straddle-mounted approach is superior - especially in a situation where the desired applied load capability is high.

Plasma Sprayed
Ceramic Coated Shaft



Test
Disk

Test Disk and Support Shaft



Slip Ring

Electrically
Conducting
Wire Through
Shaft

Support Bearings

Figure 18 High Speed Test Disk Support Shaft

All the rotating shafts of the traction rig incorporate high precision deep grooved ball bearings. These bearings were sized to carry at least the following loads of support.

Spindle shaft:	600 lbs. maximum
Belt and pulley shafts:	150 lbs. typical

In fact, each of the bearings for this device can carry the following loads according to the manufacturer's specification:

Bearing thrust capacity:	1772 lbs.
Bearing radial capacity:	1136 lbs.

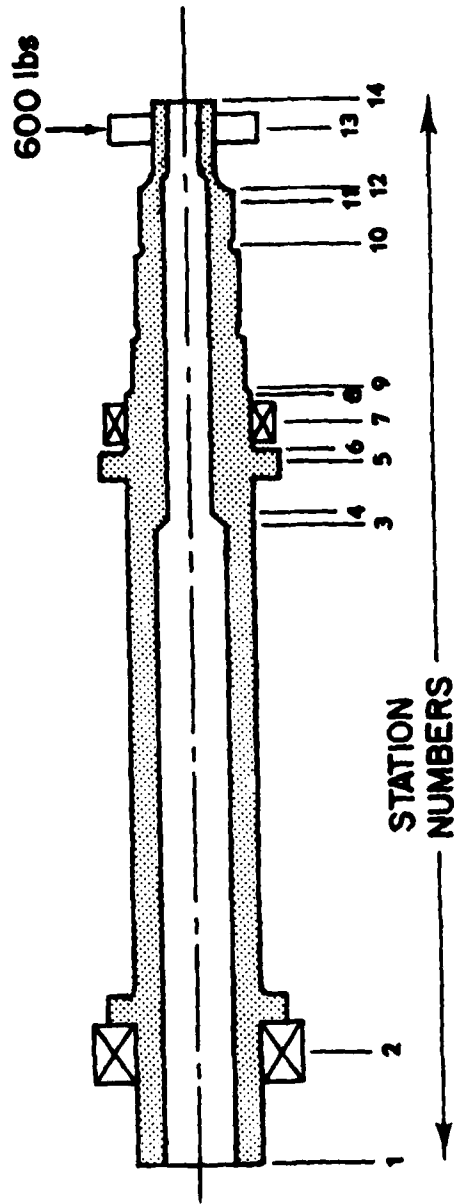
So the safety factor for all belt and pulley bearings is at least:

Bearing safety load factor:	3.8 to 1 (Pulley)
Bearing safety load factor:	1.9 to 1 (Spindle)

Part of the design study of the project included an analysis of the expected stresses to be experienced by the test support spindle under a maximum loading of 600 lbs. Figure 19 shows a test spindle cross-sectional schematic with fourteen (14) station numbers marked off along the shaft. The computed internal stresses for the shaft cross-sections at each of these stations is tabulated in Table 4 for a side load of 600 lbs on the test disk (Station 13). Note that none of the computed stress levels exceed 15,000 psi. For the shaft material of 4340 steel alloy the yield strength is given by the manufacturer as 139,000 to 165,000 psi. Therefore, the safety factor for the shaft stresses are eight-to-one or more.

The rotating speeds and sizes of the test disk spindle shafts of the traction rig are such that two important aspects of their dynamic nature must be considered; i.e.

**TEST SPINDLE SCHEMATIC
(NOT TO SCALE)**



MATERIAL 4340 HEAT TREATED

Figure 19

TABLE 4
SUMMARY TABLE OF SPINDLE STRESSES*

<u>STATION NUMBER</u>	<u>POSITION FROM 1 INCHES</u>	<u>STRESS IN lbs/ins²</u>	<u>SLOPE (RAD, IN/IN)</u>	<u>DEFLECTION IN (MILS)</u>
1	0	0	-.000525	.52
2	1	0	-.000525	0
3	6.6	5201	.000398	-1.2
4	6.7	5142	.000431	-1.1
5	7.6	9058	.000701	-.69
6	7.7	14368	.000766	-.60
7	8.3	13657	.00132	0
8	8.8	12020	.00177	.81
9	8.8	13208	.00182	.92
10	9.4	6145	.00226	2.0
11	9.8	5816	.00246	3.1
12	9.9	9964	.00251	3.3
13	10.	0	.00269	4.3
14	10.	0	.00273	5.4

* Load of 600 lbs @Station 13

1. The final shaft balancing limits, and
2. The critical speed associated with the designed shaft geometries and mass distributions.

The balancing aspects are stringent but straightforward, and the limits for this design are contained in the drawings of the rig itself.

The critical speeds of the shaft designs are more involved and the results of the analysis performed with the aid of the computer program are given in Table 5. Shown in that table is the fact that all four groups of shafts in the assembly have computed first critical speeds greater than the operating speed of the system. In particular it should be noted that the "Midspeed Shafting" and "High Speed Shafting" have computed critical speeds greater than four (4) and two (2) times running speed, respectively.

Since the computed values of critical speed are greater than any intended operating speed, it can be expected that there will be no "self-excited" instability in the rotating machinery.

d. Loading Mechanism

Three methods were considered for applying load to the test disks. These were deadweight, hydraulic, and pneumatic. Of the three, pneumatic loading was selected as the operational one to use.

Deadweight loading is ideally the most accurate and conceptually the simplest approach to static load application. However, when one considers the high speed and the inherent disk surface runout (relative to the rotational centers) one must be aware of the potential of dynamic forces being imposed upon the disk contact as inertial loading increases. Deadweight loading was given up in the present design in order to keep the overall test structure as small as possible.

TABLE 5

CRITICAL SPEED ANALYSIS SUMMARY
(1st CRITICAL IN RPM)

DESCRIPTION	MAXIMUM SPEED	FINAL DESIGN CONCEPT
MIDSPEED SHAFT	9,600	52,511*
HIGH SPEED SHAFT	24,000	48,487
HIGH SPEED SPLINE	24,000	29,094
HIGH SPEED SUPPORT SPINDLE	24,000	42,726

NOTE: ALL SECOND CRITICALS > 61,000

* : WITH COUPLING REMOVED

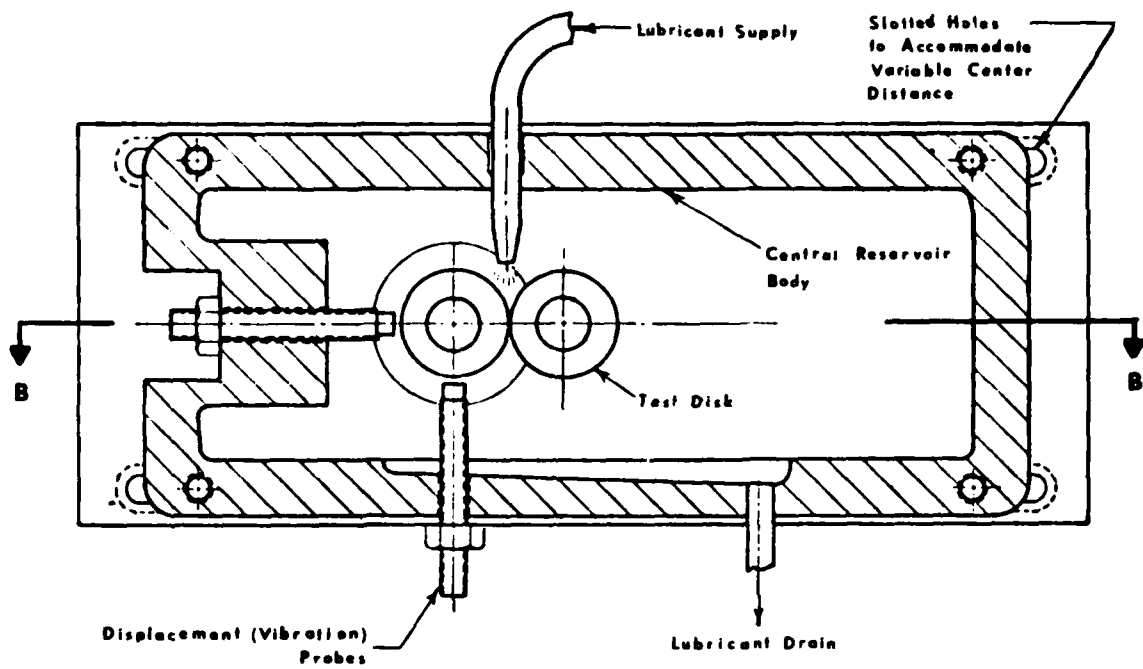
The loading mechanism selected was a pneumatic cylinder with a translatable spindle support structure with motion in the horizontal plane. This approach minimized the support housing mass yet retained the 600 lb. loading capability. An additional feature of this approach includes the placement of the load cell measuring sensor between the load point and the stationary reaction spindle for accurate determination of disk loading. This also provided a long-length stroke mechanism which can be easily moved "out of the way" during maintenance periods.

e. Test Disk Enclosure and Lubricant Circulating System

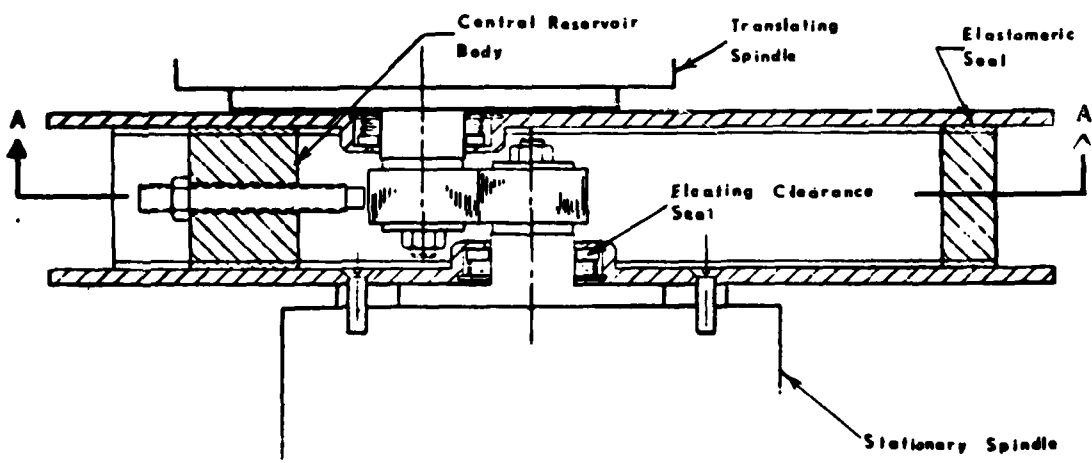
The test disk enclosure was designed to incorporate the following primary requirements:

- it had to be reasonably well sealed to prevent loss of lubricant;
- it could not trap lubricant;
- it had to be easy to disassemble for disk replacement;
- different shaft center distances had to be accommodated;
- it had to accommodate and support test lubricant plumbing;
- it had to be made of materials that were compatible with a wide variety of traction lubricants.

The enclosure concept is shown schematically in Figure 20. It consists of two plates which contain the spindle shaft seals, a central reservoir body, and two elastomeric Viton seals for statically sealing the plates to the reservoir body. This body is used for many functions and supports the disk displacement (vibration) probes, the lube supply nozzle, and the lube drain plumbing. Each plate contains one self-centering close clearance carbon shaft seal which accommodates machinery tolerance stock-ups and the small radial shaft displacement that will be encountered during a test sequence. Center



SECTION A-A



SECTION B-B

Figure 20 Schematic of Test Disk Enclosure

distance accommodation is accomplished by changing the relative location of the two plates through the slotted bolt holes that attach the plates to the central reservoir body.

The floating close clearance shaft seals have a large clearance around their O.D.'s and are held in place by light axial springs. They are restrained from rotation by an anti-rotation pin.

One of the plates is secured to the stationary (non-translating) spindle. To change disks, the screws that secure the central reservoir body are removed, one then rotates the reservoir about 60° and then the translating spindle is moved away from the stationary spindle (by retracting the pneumatic loading piston). During this process the central body moves with the translating disk exposing it for servicing. There is working room inside the central reservoir body for removal of the disk.

The test disk enclosure is connected through plastic tubing to the test lubricant pumping and temperature control loop. A peristaltic-type variable speed circulating pump is incorporated. The test lubricant flow/control components are attached to the central test apparatus base supporting structure.

f. Drive Motors

The requirements of a traction test device impose stringent requirements on the drive motors. They must have smooth variable speed capability which is easily controllable. They have to be able to absorb power as well as produce it. Furthermore, the change from the power producing mode to the power absorbing mode must be inherently automatic; i.e., external switching to accomplish the mode change is possible.

Silicon-controlled rectifiers (SCR) for adjustable speed motor drives accomplish the above requirements and have been widely accepted by the production industry for many years. There are at least ten manufacturers of standard SCR drive systems that are suitable for the traction rig application. SCR drives provide low maintenance and highly reliable performance over a variable speed range of about twenty-to-one. The typical SCR package contains a DC motor, a power conversion unit, and an operator's control that is usually small and easy to use. The operator's control usually contains a start/stop button and a motor speed adjusting rheostat.

The drive motors selected to power the traction disk have inherent regenerative power feedback for proper traction curve production. Since the two traction disks alternately transfer power from one to another as the slip speeds are varied through speed adjustments, each motor must be able to absorb power (act as a brake) or supply power. The term regeneration describes this mode of operation. The regeneration capability is generally an optional feature that can be purchased with rectifier drives.

Rectifiers allow current to flow in only one direction, and special circuitry is required to provide for normal motoring as well as regeneration. A "back-to-back" armature rectifier circuit has important advantages in that it allows maximum dynamic response and non-contactor reversing.

The basic unit picked for the traction drive application has "regenerative" capability, as well as the following features:

- 2 - 10 Horsepower D.C. motors
- 2 - SCR power control units
- 2 - operator's controllers with start/stop and speed adjustment controls

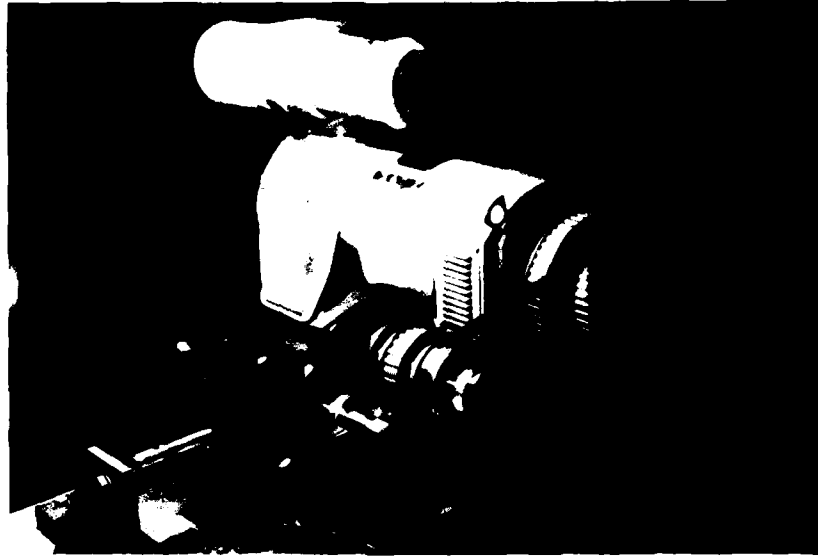
- 20:1 full torque speed range (2500 RPM max. speed)
- 460 volts input powering
- 50 to 60 cycle current
- less than a 2% speed drop with a 0 to 75% change of full load.

One of the twin ten horsepower motors and its associated drive transmission is shown in the upper photo of Figure 21. The minimum horsepower required for the motor-controller is shown in the schematic of Figure 22. That figure also gives the proper input power line phasing and wire color codes for the installed system. When connected in the manner shown, proper shaft rotation for testing will result.

g. Instrumentation for Data Monitoring

The tests to be monitored in the traction apparatus require a variety of electronic sensing, conditioning and display outputs. Each of the signal functions to be monitored with the aid of the small traction apparatus instrument panel are tabulated in Table 6.

Signals generated from the apparatus disk load, lubricant temperature, speed, torque, film, and vibration are provided in the modes listed. In general, the techniques chosen for each of these measurements involve the use of standard electronic methods. Load and torque measurements make use of strain gage technology for primary sensing. Temperatures are obtained via thermocouple point sensing in either the lubricant fluid streams or the body of the test rig support structures. Disk speeds are determined analytically with the aid of a digital electronic system which uses a five megahertz oscillator and timing markers on each rotating shaft. Contact disk film monitoring is accomplished in the rotating disk assembly through built-in slip rings. Contact resistance is measured with a low voltage (about .1 volt) applied across the rotating disks during measurement. Vibration is obtained with piezoelectric sensors and inductive displacement sensors. The appropriate number of each type of sensor is shown in Table 6.



Ten Horsepower Drive Motor on Base



Figure 21 Transmission Shafting

TABLE 6

SMALL TRACTION APPARATUS SIGNAL CONDITION MONITORS PROVIDED

SIGNAL FUNCTION MONITORED	NORMAL DISK LOAD	LUBRICANT TEMPERATURE			DISK SPEEDS		DISK SHAFT TORQUE	FILM CONDITION	VIBRATION	
		Test Lub	Shaft Brgs.	Switch	Running	Slip			Displacement	Accelerometer
DESCRIPTION	Load Cell							Electac		
TECHNIQUE USED	Strain Gage	T/C	T/C	T/C	Pulse Counting	Pulse Diff.	Strain Gage	Electrical Resistance	Inductive	Piezo electric
NUMBER OF SIGNALS	1	2	2	6	1	2	1	1	2	2
PRIMARY SENSOR(S) NEEDED	•	•	•	•	•	•	•	None but Slip Rings Supplied	•	•
ELECTRONIC CONDITIONER	•	•	•	•	•	•	•	•	•	•
DIGITAL VISUAL DISPLAY	•	•	•	•	•	•	•			
NEEDLE METER DISPLAY								•		
ANALOG SIGNAL AVAILABLE	•	•	•	•	•	△	△	•	•	
SCANNED DATA LOGGER SIGNALS IN HARD COPY AVAILABLE	•	•	•	•	•	•	•	•	•	•

△ = Attached to Realtime Data X-Y Plotter

• = Yes

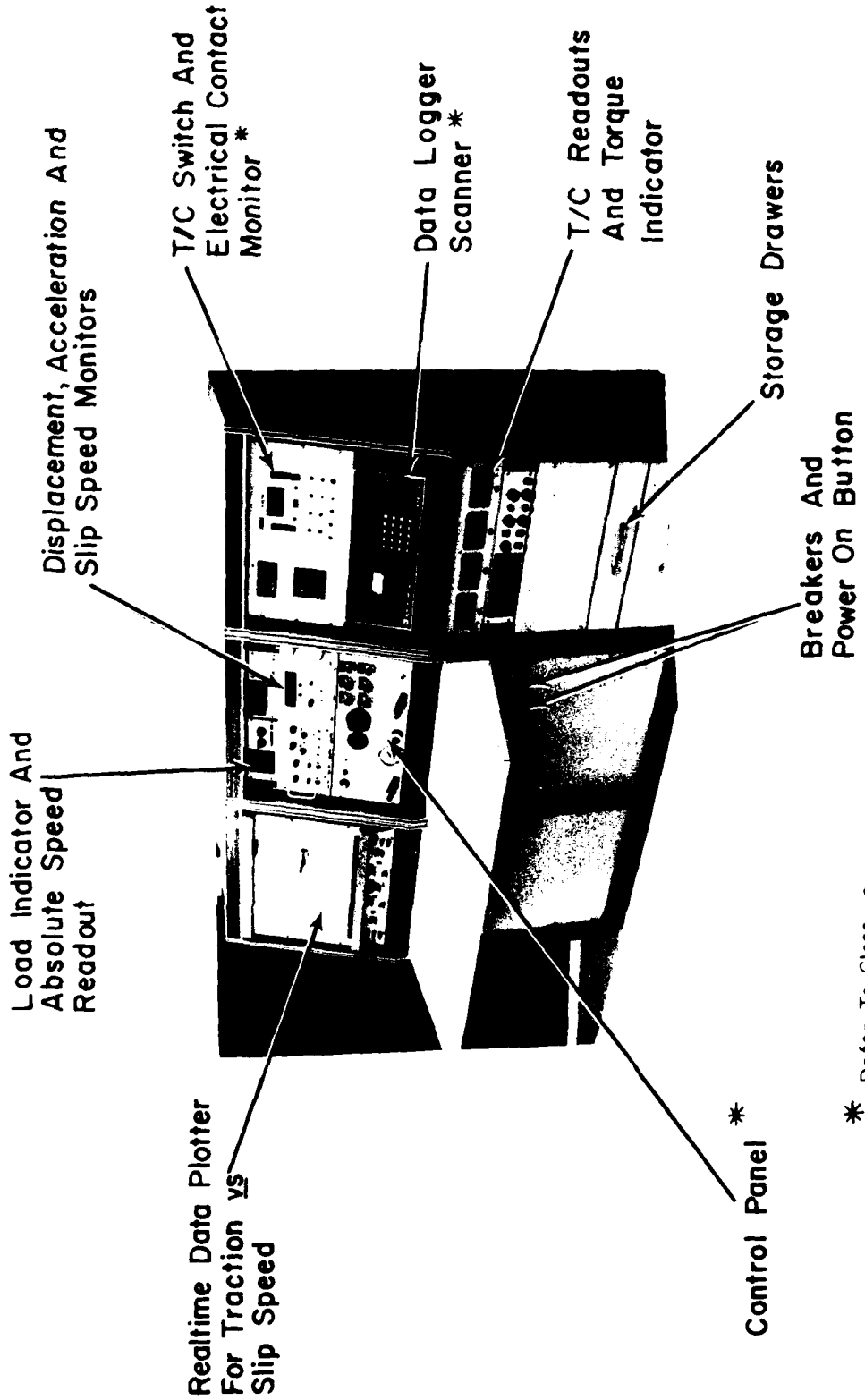
Blank = Not provided

Each type of sensor has an excitation and electronic conditioning unit provided. Output signals are provided in the proper engineering units for each interpretation where needed. Figures 23 through 25 contain photographs of the instrumentation panel with annotated close-ups of the signal conditioning and monitoring electronics.

The system incorporates a programmable scanning device which provides the hard copy display if needed for test recording. The data logger although not interfaced with a computer could be in the future with the addition of appropriate electronic optional cards. A sample printout of the type of scanner data available is shown in Figure 26.

h. Control Panel Layout

Figure 27 is an annotated photographic close-up of the control panel portion of the test rig instrument system. Depicted are the twin 10 horsepower start/stop buttons, multi-turn motor speed control rheostats, lubricant pumping controls, sump temperature controller, pressure of lubricant supply, pressure gage of load cell pneumatic cylinder, and keyed A.C. panel power on/off switch.



* Refer To Close-up Of Additional Figure Detail

Figure 23 Instrument Control and Monitor Panels

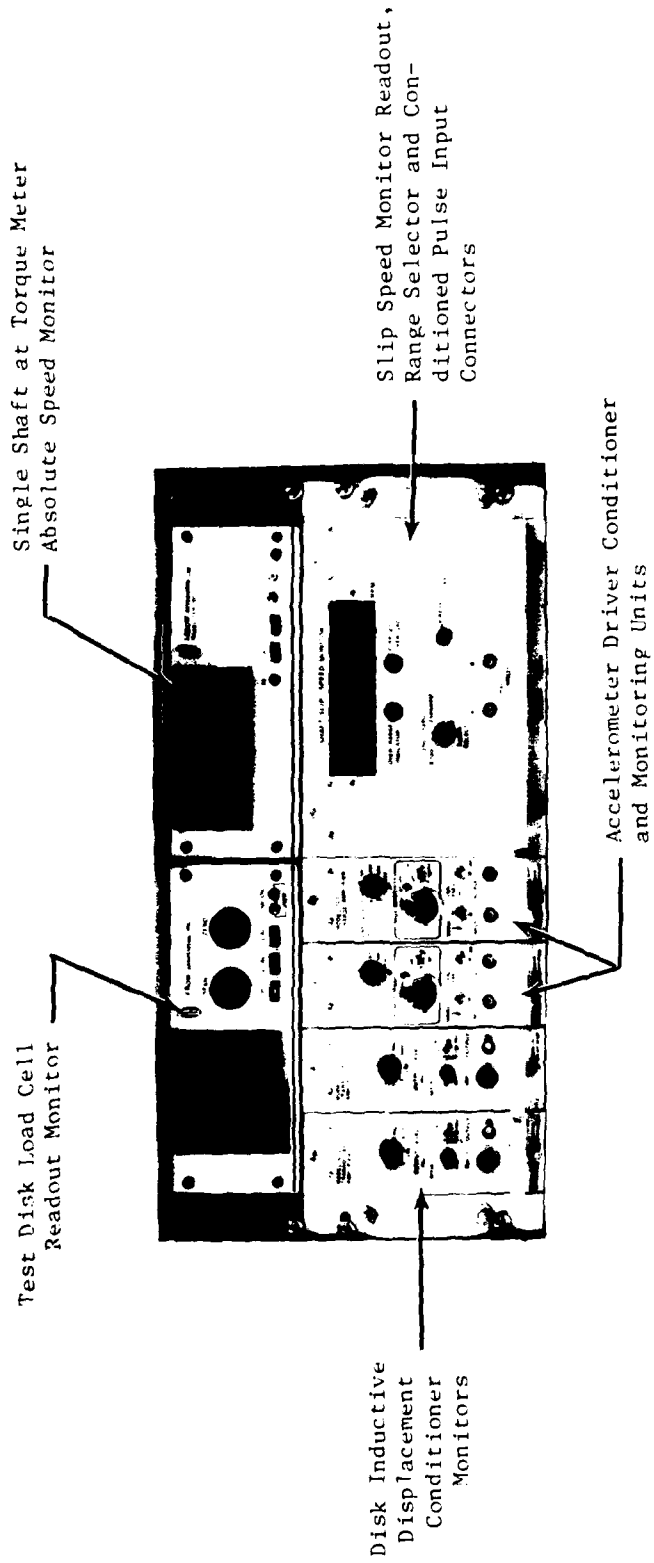


Figure 24 Instrument Monitors for Load, Slip Speed, Displacement

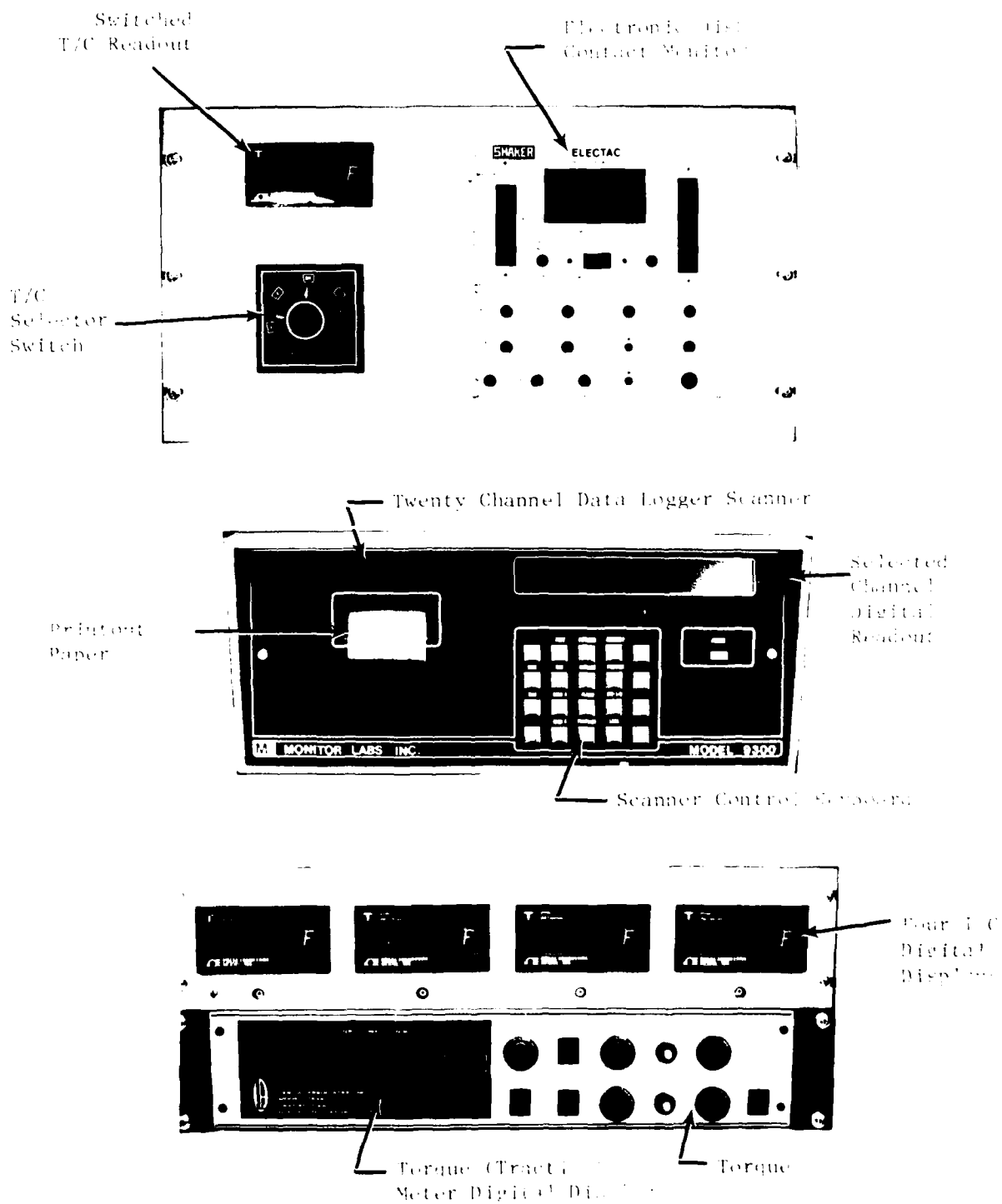


Figure 25 Instrument Monitors for Temperature, Electrical Contact Torque (Traction), and Data Logging (Full Right Side View of Instrument Panel)

LOGGER PROGRAM USED
TO PRINTOUT

SAMPLE DATA
LOGGER OUTPUT
FORMAT

2 0.6766LBS
1 19276RPM
0 0.0099TDR
000:03:21:37

2 0.6766LBS
1 19276RPM
0 0.0099TDR
000:03:21:35

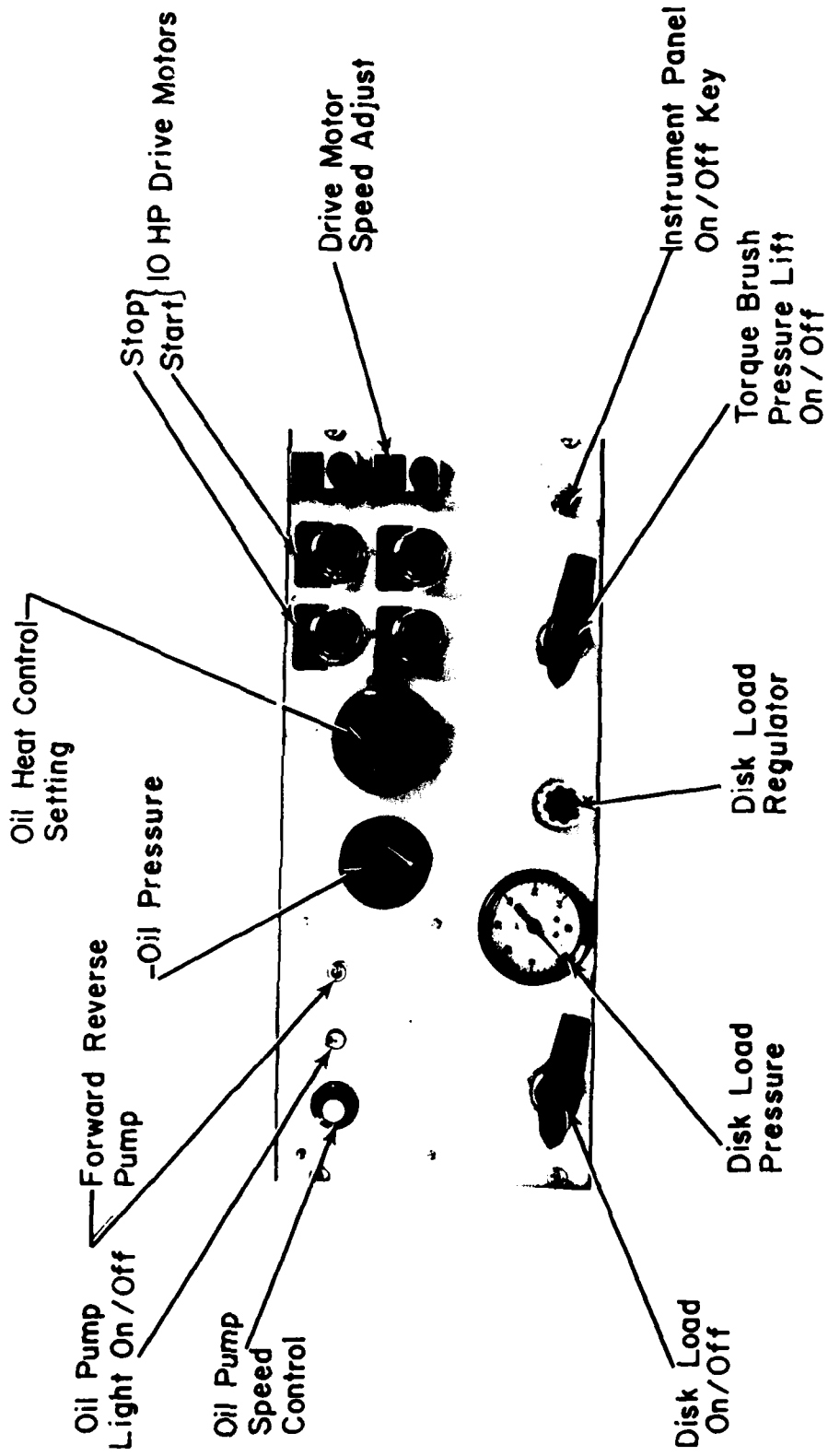
PRT INST? YES
B= 0
M= 200
DDM= 161
RGE= 3Y
SKIP? NO
CHANNEL= 2

PRT INST? YES
B= 0
M= 10000
DDM= 180
RGE= 3Y
SKIP? NO
CHANNEL= 1

PRT INST? YES
B= 0.3575
M= 33.47
DDM= 215
RGE= 3Y
SKIP? NO
CHANNEL= 1

DATE INFORMATION
Day:Mo:Hr:Min

Figure 26 Sample Data Logger Printout



CONTROL PANEL

Figure 27 Control Panel Layout Details

3.0 REFERENCES

1. Smith, R. L., Walowit, J. A., and McGrew, J. M., "Elastohydrodynamic Traction Characteristics of 5P4E Polyphenyl Ether," *Journal of Lubrication Technology*, Trans. ASME, Series F, Vol. 95, No. 3, July, 1973.
2. Walowit, J. A., and Smith, R. L., "Traction Characteristics of a MIL-L-7808 Oil," ASME Paper No. 76-LUBS-19, presented at the Lubrication Symposium, Atlanta, Georgia, May 24-26, 1976.
3. Misharin, J. A., "Influence of the Friction Conditions on the Magnitude of the Friction Coefficient in the Case of Rolling with Sliding," *Proceedings of the International Conference on Gearing*, The Institute of Mechanical Engineers, London, 1958, pp. 159-164.
4. Benedict, G. H., and Kelley, B. W., "Instantaneous Coefficients of Gear Tooth Friction," *Trans. ASLE*, Vol. 4, 1959.
5. Crook, A. W., "The Lubrication of Rollers. III. A Theoretical Discussion of Friction and the Temperatures in the Oil Film," *Phil. Trans. Roy. Soc. Londong*, A254, p. 237, 1961.
6. Crook, A. W., "The Lubrication of Rollers - IV Measurements of Friction and Effective Viscosity," *Philosophical Trans. Series A* 255, 281.
7. Smith, F. W., "Lubricant Behavior in Concentrated Contact -- Some Rheological Problems," *Trans. ASLE*, 3 (1), pp. 18-25, 1960.
8. Hewko, I. O., Rounds, F. G., and Scott, R. I., "Tractive Capacity and Efficiency of Rolling Contacts," in Rolling Contact Phenomena. Editor, J. B. Bidwell, Elsevier, New York, 1962.
9. Smith, F. W., "Rolling Contact Lubrication - The Application of Elastohydrodynamic Theory," *J. of Basic Engrg*, Trans. ASME, Vol. 87, Series D, No. 1, March 1965, p. 170.
10. Wernitz, W., "Friction at Hertzian Contact with Combined Roll and Twist" in Rolling Contact Phenomena. Editor, J. B. Bidwell, Elsevier, New York, 1962.
11. Bell, J. C., Kannel, J. W., and Allen, C. M., "The Rheological Behavior of the Lubricant in the Contact Zone of a Rolling Contact System," *J. Basic Engrg.*, Trans. ASME 86, Series D, No. 3, p. 423, 1964.
12. Fein, R. S., "Possible Role of Compressional Viscoelasticity in Concentrated Contact Lubrication," *Trans. ASME, J. Lub. Tech.*, Vol. 89F, pp. 127-133, 1967.

13. Johnson, K. I. and Cameron, R., "Shear Behavior of Elastohydrodynamic Oil Films at High Rolling Contact Pressures," Proc. Inst. of Mech. Eng., London. 182, Part I, pp. 307-330, 1967-68.
14. Dyson, A., "Frictional Traction and Lubricant Rheology in Elastohydrodynamic Lubrication," Proc. Roy. Soc., London. 266A, p. 1, 1970.
15. Kannel, J. W., and Walowit, J. A., "Simplified Analysis for Traction between Rolling Sliding Elastohydrodynamic Contacts," Trans. ASME, J. of Lubr. Tech., January, 93, p. 39, 1971.
16. Harrison, G. and Trachman, E. G., "The Role of Compressional Viscoelasticity in the Lubrication of Rolling Contacts," Trans. ASME, J. of Lubr. Tech. 94, Oct., p. 306, 1972.
17. Trachman, F. G. and Cheng, H. S., "Thermal and Non-Newtonian Effects on Traction in Elastohydrodynamic Contacts," Proc. Inst. Mech. Engrs., "Elastohydrodynamic Lubrication: 1972 Symposium, p. 142, 1972.
18. Johnson, K. I., and Roberts, A. D., "Observations of Viscoelastic Behavior of an Elastohydrodynamic Lubrication Film," Proc. R. Soc. Lond. A337, pp. 217-242, 1974.
19. Hirst, W. and Moore, A. J., "Non-Newtonian Behavior in Elastohydrodynamic Lubrication," Proc. R. Soc., London. A337, pp. 101-121, 1974.
20. Lingard, S., "Traction at the Spinning Point Contacts of a Variable Ratio Friction Drive," Tribology Intl., October, p. 228, 1974.
21. Bair, S. and Winer, W. O., "A Rheological Model for Elastohydrodynamic Contacts Based on Primary Laboratory Data," ASME Paper 78-Lub-9.
22. Daniels, B. K., "Non-Newtonian Thermo-Viscoelastic EHD Traction from Combined Slip and Spin," ASLE Paper 78-LC-2A-2.
23. Smith, R. L., et al., "Research on Elastohydrodynamic Lubrication Rolling-Sliding Contacts," Air Force Aero Propulsion Laboratory, AFAPL-TR-72-56, July 1972.
24. Smith, R. and McGrew, J. M., "Accelerated Life Testing of Despun Antenna Bearings," Final Report prepared under Communication Satellite Corporation, Contract No. CSC-SS-228, October 1971.
25. Smith, R. and McGrew, J. M., "Failure Modes and Accelerated Life Test Methods for Despun Antenna Bearings," Lubrication Engineering, Vol. 30, No. 1, January 1974.
26. McGrew, J. M., et al., "Elastohydrodynamic Lubrication - Preliminary Design Manual," Air Force Systems Command, AFAPL-TR-70-27, November, 1970.

27. Smith, R. L., Walowit, J. A., and Pan, C. H. T., "High Pressure Pulsed Capillary Viscometry," NASA Report C120982, prepared under Contract NAS3-14419, August, 1972.
28. Johnson, K. I. and Tevaarwerk, J. I., "Shear Behavior of Elastohydrodynamic Oil Films," Proc. R. Soc. Lond. A356, p. 215, 1977.
29. MIL-STD-882, "Requirements for: System Safety Program for Systems and Associated Subsystems and Equipment," July 15, 1969.
30. Smith, R. L., "System Safety Program Plan and Hazard Analysis Report for Small Traction Apparatus Development Project," under WPAFB Contract F33615-79-C-5051, April, 1980.
31. Smith, R. L., "Operations Manual of the Development of a Lubricant Traction Measuring Device," Contract Report AFML-TR-81-XX, 1981.
32. Smith, R. L., "Maintenance Manual of the Development of a Lubricant Traction Measuring Device," Contract Report AFML-TR-81-XX, 1981.

APPENDIX I

TRACTION APPARATUS DESIGN DRAWINGS LIST

ASSEMBLY DRAWINGS

<u>DRAWING NUMBER</u>	<u>DESCRIPTION</u>
J-100 (Sheet 1 & 2)	General Assembly
D-200	Shaft Extension Assembly
D-300	Belt Adjuster Assembly
J-400 (Rev. B)	High Speed Shaft Assembly
J-500 (Rev. B)	Support Spindle Assembly
D-600 (Rev. B)	Test Enclosure Assembly
D-9()	Water Heater Tank
D-1000 (Rev. A)	Heat Exchanger

TOOL DRAWINGS

<u>DRAWING NUMBER</u>	<u>DESCRIPTION</u>
B-700	Specimen Tool (Male)
B-701	Specimen Tool (Female)
B-702	Belt Tightening Bar
B-703	Nut Wrench
B-704	Puller Body
B-705	Puller Ears
C-706	Half Keys (Balancing)
A-707	Belt Tensioning Curve

BALANCING DRAWINGS

<u>DRAWING NUMBER</u>	<u>DESCRIPTION</u>
D-800	Support Spindle
D-801	Spindled Shaft
D-802	Low-Speed Shaft
D-803	Mid-Speed Shaft
D-804	High-Speed Shaft

BALANCING DRAWINGS (cont.)

<u>DRAWING NUMBER</u>	<u>DESCRIPTION</u>
B-001	Shaft Extension
B-002	Sleeve/Inner Race
B-003	Outer Race Clamp
C-004	Transmission Cover
B-005	Low-Speed Shaft
B-006	Mid-Speed Shaft
C-007	Pulley-Flat Belt
C-008	Timing Belt Pulley (Mod)
B-009	Coupling Detail
B-010	Outer Race Clamp
C-011	Keys - Half
C-012	Guide 45°
D-013	Bearing Support (Mid-Speed)
D-014	High-Speed Housing Machining
J-015	Housing Slide
D-016	Bearing Hub
D-017 (Rev. A)	Cooling Jacket
D-018	High-Speed Shaft
D-019	Inboard Split Plate
D-020	Bearing Support (Low-Speed)
B-021	Retainer-Inboard
B-022 (Rev. B)	Retainer-Outboard
B-023	Connector Pin
C-024	Spring Housing
B-025	Plunger
D-026	Bracket Weldment
B-027	End Plate - Spring Housing
B-028	Nut/High-Speed Shaft
D-030 (Rev. A)	Shaft (Assembly/Machining)

BALANCING DRAWINGS (cont.)

<u>DRAWING NUMBER</u>	<u>DESCRIPTION</u>
C-031	Shaft (with internal spline)
D-032	Bearing Support Housing
B-033	Ext. Splined Sleeve
D-034 (Rev. A)	Inboard Housing
D-035 (Rev. A)	Outboard Housing
B-036 (Rev. A)	Bearing Spacer
C-037	Cooling Jacket (Translating)
C-038	Cooling Jacket (Stationary)
B-039	Insulated Washer
B-040 (Rev. A)	Inboard Solder Ring
B-041	Bearing Nut Modification
B-042	Insulating Washer
B-043	Retainer Sleeve
B-044	Positioning Screw
B-045	Inboard Outer Race Clamp
B-046	Anti-Rotation Screw
B-047	Jacking Collar
B-048	Outboard Solder Ring
B-049	Cover Plate
B-050 (Rev. A)	Outboard Washer
B-051	Outboard Bearing Spacer
B-052	Face Plate
C-054	Specimen
D-057	Mounting Cradle
D-058	Inboard Mounting Bracket
C-059	Outboard Mounting Bracket
D-060 (Rev. A)	Split Shaft (Outboard)
D-061	Split Shaft (Inboard)
D-062	Tie Bolt
D-065 (Rev. A)	Reservoir
C-066	Face Plate (Stationary)
C-067	Face Plate (Translating)

BALANCING DRAWINGS (cont.)

<u>DRAWING NUMBER</u>	<u>DESCRIPTION</u>
B-068	Gasket (Stationary)
B-069	Gasket (Translating)
C-070	Seal Housing
B-071	Sealing Plate
B-072	Cover Plate
B-073	Seal
B-074	Pressure Plate
B-075	Spray Bracket
B-081	Shaft Actuator
B-082	Load Cell Adapter
B-084	Shaft Way
B-085	Support Mount Plate (Type A)
B-086	Support Mount Plate (Type B)
C-087	Traction Rig Console
B-088 (Sheet 1 - 4)	Model 701 Charge Amplifier
A-089	Model 701 Charge Amplifier Wiring Diagram
A-090	Panel Layout
A-091	Panel Drill Drawing
D-093	Motor Mount
J-094	Outboard Sub-structure
J-095	Inboard Sub-structure
C-096	Shaft Way
B-097	Way Support (Type A)
B-098	Way Support (Type B)
B-099	Way Clamp
C-101	Hand Wheel
C-102	Shaft
B-103	Mounting Bracket
B-104	Threaded Sleeve
J-105	Transmission Mount (Stationary)

BALANCING DRAWINGS (cont.)

<u>DRAWING NUMBER</u>	<u>DESCRIPTION</u>
B-106	Key (Spindle)
J-107	Translating Transmission Mount
C-108	Coupling Guard
B-110	Tensioning Brace
C-111	Fiber Optic Scanner Amplifier/ Line Driver
A-112	Wire Wrap Board
D-113	Differential Speed CKT
C-114	Differential Speed Assembly Front & Rear Panel Drill Drawing
C-116	Differential Speed Assembly Front Panel Silkscreen Layout
D-119	Console to Rig Connection Diagram
D-120	Electac Front Panel Drilling

APPENDIX II

LIST OF INSTRUMENTATION MONITORING EQUIPMENT

LIST OF INSTRUMENTATION MONITORING EQUIPMENT

<u>Quantity Required</u>	<u>Description</u>
1	Load Cell (Strain Gage), Lebow 31321K
1	Strain Gage Conditioner/Indicator, Lebow 7530-103
1	Hard Copy Data Logger, Monitor Labs #9300 (20 channels)
10	Thermocouples (Wire), Omega NW-T-24
1	Thermocouple (Switch), Omega #YSTR3-06
5	Thermocouple Conditioner/Indicator, Omega MOD 199
2	Photo Optic Sensor, SKAN-A-Matic 5322-3
1	Slip Speed Monitor
1	Absolute Speed Indicator, Lebow 7215-103
1	Torque Meter, Lebow #1115A
1	Torque Indicator/Conditioner, Lebow #7535
2	Slip Rings, Airflyte Electronics BSR-1358-4
2	Brush Block, Airflyte Electronics BBK-1183-4
2	Vibration Displacement Sensor, Bently #300H
2	Vibration Accelerometer, B & K #4344
2	Induction Probe Drivers, Shaker 502
1	Accelerometer Excitation, Shaker 701
1	Plotter X-Y Recorder, MFE 815XY Plotter
1	Electrical Contact Monitor, Shaker #301
1	Adtech Power Line Conditioner Model PEC-500

APPENDIX III

SAMPLE DATA SCANNER PROGRAM LISTING

SAMPLE SCANNER PROGRAM LISTING

(Full Program 10 Channels)

On Next Page

PROGRAM LISTING

Logger
Output
PRINTOUT

2 0.6766LBS
1 19276RPM
0 0.0099TOR
000:03:21:37

2 0.6768LBS
1 19277RPM
0 0.0099TOR
000:03:21:35

PRT INST? YES
B= 0
M= 200
CONV= 161
RGE= 3V
SKIP? NO
CHANNEL= 2

PRT INST? YES
B= 0
M= 10000
CONV= 180
RGE= 3V
SKIP? NO
CHANNEL= 1

PRT INST? YES
B= 0.3575
M= 35.47
CONV= 215
RGE= 3V
SKIP? NO
CHANNEL= 0

DATE INFORMATION
Day:Mo: Hr:Min

SAMPLE PROGRAM

PRT INST? YES
B= 0
M= 10000
CONV= 180
RGE= 3V
SKIP? NO
CHANNEL= 3

PRT INST? YES
B= 0
M= 200
CONV= 161
RGE= 3V
SKIP? NO
CHANNEL= 2

PRT INST? YES
B= -2550
M= 500
CONV= 180
RGE= 10V
SKIP? NO
CHANNEL= 1

PRT INST? YES
B= 0.3575
M= 35.47
CONV= 215
RGE= 3V
SKIP? NO
CHANNEL= 0

ALM PRT? NO
P RATE= NO
RATE= NO
LP= 0
B FP= 0
RATE= NO
LP= 9
A FP= 0
MON CHL= 0
MON MODE 1-4= 1
P 257:14:59:13

PRT INST? YES
B= 0
M= 1000
CONV= 323
RGE= 3V
SKIP? NO
CHANNEL= 9

PRT INST? YES
B= 0
M= 1000
CONV= 323
RGE= 3V
SKIP? NO
CHANNEL= 8

PRT INST? YES
B= 0
M= 1000
CONV= 323
RGE= 3V
SKIP? NO
CHANNEL= 7

PRT INST? YES
B= 0
M= 1000
CONV= 323
RGE= 3V
SKIP? NO
CHANNEL= 6

PRT INST? YES
B= 0
M= 1000
CONV= 323
RGE= 3V
SKIP? NO
CHANNEL= 5

PRT INST? YES
B= 0
M= 1000
CONV= 323
RGE= 3V
SKIP? NO
CHANNEL= 4

APPENDIX IV

PHYSICAL PROPERTIES OF FLUID O-77-3J
LUBRICANT USED IN THIS INVESTIGATION

PHYSICAL PROPERTIES OF FLUID O-77-3J
LUBRICANT USED IN THIS INVESTIGATION

Index of Refraction ¹	1.475
Density ²	0.03326 lb/in ³
Viscosity ²	12.68 CP
Bulk Modulus ²	212962 lb/in ²
Pressure-Viscosity Coefficient ²	9.95 10 ⁻⁵ in ² /lb
Temperature-Viscosity Coefficient ²	4840 °R
Thermal Conductivity ¹	0.0558 Btu/hr/ft/°F
Specific Heat ¹	2.0 Btu/lb-°F

NOTES:

1. Value is an estimate based on values for similar oils.
2. Represents value at 100°F, atmospheric pressure based on measured values of viscosity and density of ATL-0137, a base stock used in the formulation of MIL-L-7808.

APPENDIX V

SAMPLE TRACTION VS. SLIP SPEED CURVES DATA SUMMARY

FOR

AIR FORCE CODE 0-77-3J LUBRICANT

(SEE APPENDIX IV FOR IDENTIFICATION)

DESCRIPTION OF TEST SENSORS
BY TEST CHANNEL NUMBER

<u>MONITORED TEST DATA CHANNEL NUMBER</u>	<u>TEST SENSOR DESCRIPTION</u>
8	TC5 Heater Tank
7	Switched either TC1, 2, 4, 12, 15, 16
6	TC7 High speed bearing stationary
5	TC10 High Speed Bearing translating
4	TC9 Oil inlet temperature °F
3	Torque shaft speed RPM
2	Disk Load lbs.
1	Slip speed FPM
0	Rig torque in-lbs

*

3 2195.0RPM
2-21.560LBS
1 1317RPM
0-1.4585TOR
P 257:14:35:24

RUN A

(See Run of Torque vs. Slip Speed)

3 2196.0RPM
2-20.900LBS
1 -878.0RPM
0-0.2171TOR
P 257:14:35:52

3 2198.0RPM
2-101.18LBS
1 -858.5RPM
0 0.7051TOR
P 257:14:37:00

3 2209.0RPM
2-100.72LBS
1 1119RPM
0-3.1425TOR
P 257:14:37:46

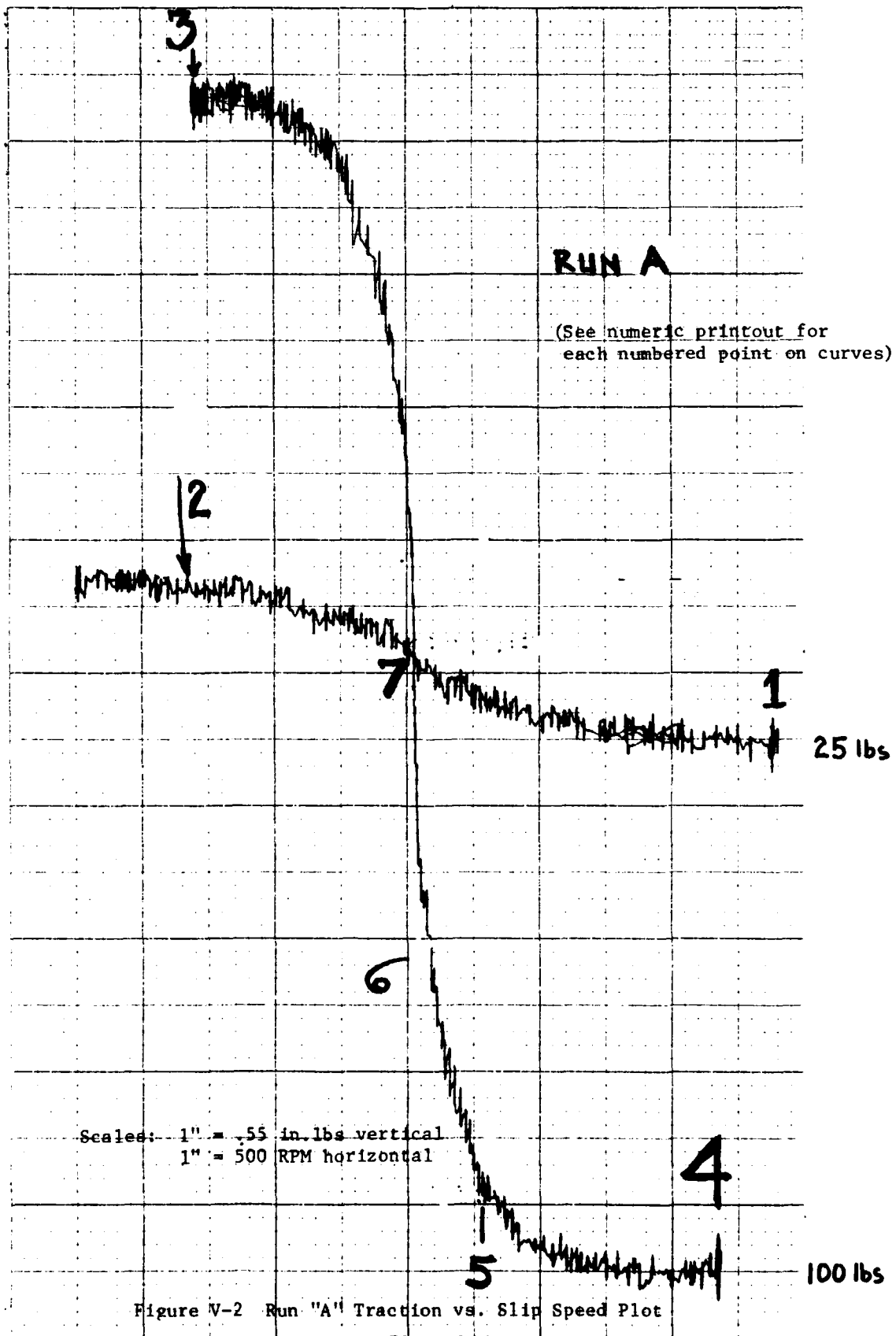
3 2208.0RPM
2-100.56LBS
1 293.0RPM
0-2.3453TOR
P 257:14:38:03

3 2241.0RPM
2-100.30LBS
1 30.5RPM
0-1.1286TOR
P 257:14:38:18

3 2206.0RPM
2-100.38LBS
1 -25.0RPM
0-0.5469TOR
P 257:14:38:28

* See explanation of channel numbers

Figure V-1 Run "A" Data Scanner Printout



3 5007RPM
 2-30.040LBS
 1 89.0RPM **8**
 0-1.6146TOR
 P 257:14:42:28

RUN B

(See Run of Torque vs. Slip Speed)

3 5007RPM
 2-30.040LBS
 1 89.0RPM **9**
 0-1.6146TOR
 P 257:14:42:55

3 5011RPM
 2-30.040LBS
 1 -854.5RPM **10**
 0-0.6924TOR
 P 257:14:43:24

3 5019RPM
 2 -60.26LBS
 1 1516RPM **11**
 0-1.4550TOR
 P 257:14:45:09

3 5020RPM
 2 -59.32LBS
 1 -10.5RPM **12**
 0-0.5682TOR
 P 257:14:45:25

8 70.30°F
 7 84.30°F
 6 81.40°F
 5 84.10°F
 4 86.30°F
 3 0.000RPM
 2 0.000LBS

3 5016RPM
 2 -58.32LBS **13**
 1 -482.0RPM
 0-0.5860TOR
 P 257:14:45:47

* See explanation of channel numbers

Figure V-3 Run "B" Data Scanner Printout

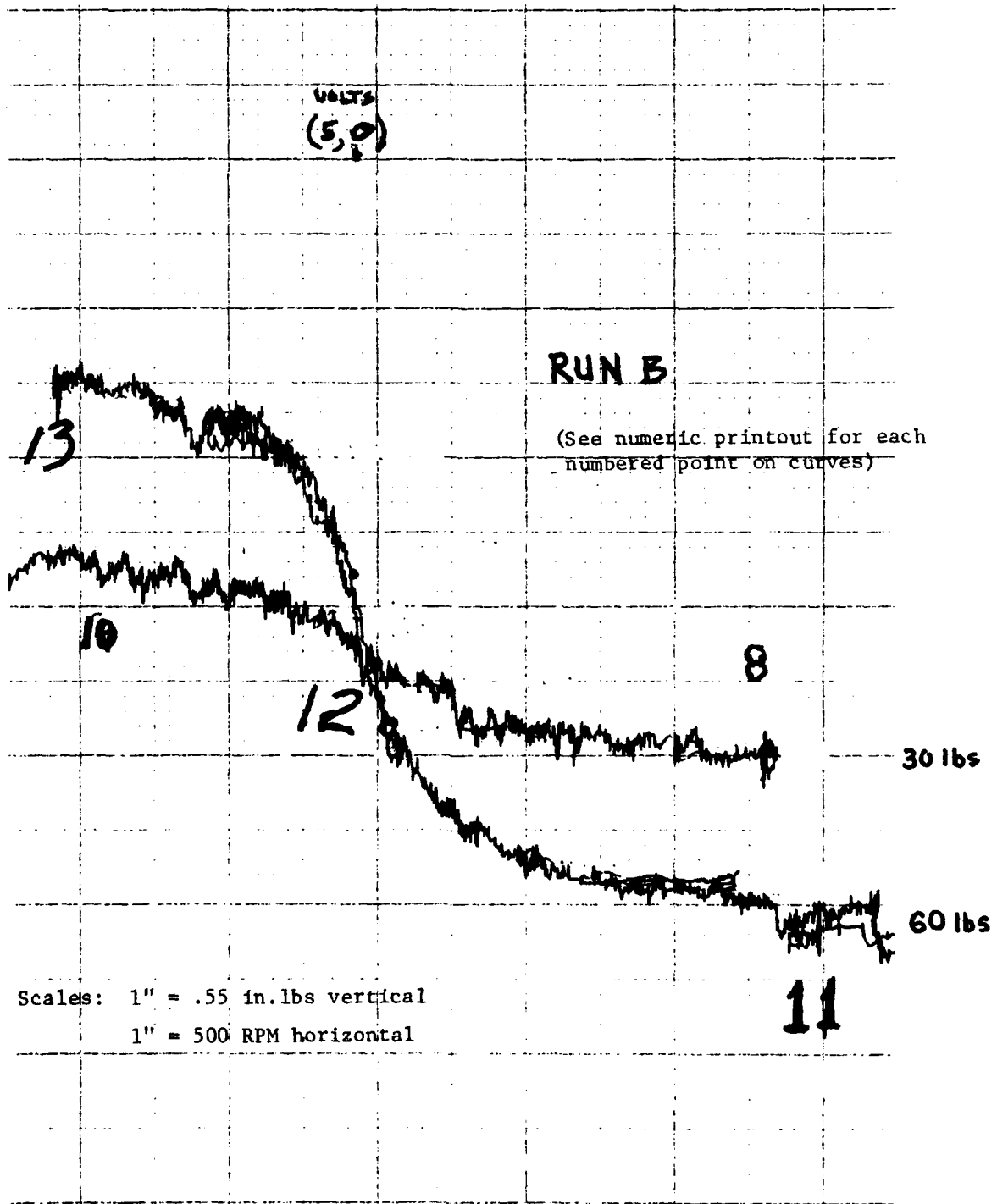


Figure V-4 Run "B" Traction vs. Slip Speed Plot

RUN 1

(See Run of Torque vs. Slip Speed)

9 70.70°F 1
 8 71.00°F
 7 74.50°F
 6 77.50°F
 5 79.10°F
 4 80.00°F
 3 3274.0RPM
 2-30.580LBS
 1 958RPM
 0-1.1689TDR
 P 261:14:37:59

9 66.90°F 2
 8 71.40°F
 7 74.80°F
 6 78.00°F
 5 80.00°F
 4 80.80°F
 3 2299.0RPM
 2-31.180LBS
 1 -28.0RPM
 0-0.8236TDR
 P 261:14:39:00

9 73.50°F 3
 8 71.00°F
 7 74.60°F
 6 78.10°F
 5 79.30°F
 4 81.30°F
 3 1601.0RPM
 2-31.780LBS
 1 -736.0RPM
 0-0.3412TDR
 P 261:14:39:43

9 74.20°F 4
 8 71.00°F
 7 74.70°F
 6 78.30°F
 5 79.70°F
 4 82.60°F
 3 2329.0RPM
 2-34.580LBS
 1 795RPM
 0-1.8942TDR
 P 261:14:41:13

9 69.50°F 5
 8 71.50°F
 7 82.20°F
 6 78.80°F
 5 81.50°F
 4 83.10°F
 3 2287.0RPM
 2-31.440LBS
 1 -980.0RPM
 0-0.8082TDR
 P 261:14:42:06

* See explanation of channel numbers

Figure V-5 Run "1" Data Scanner

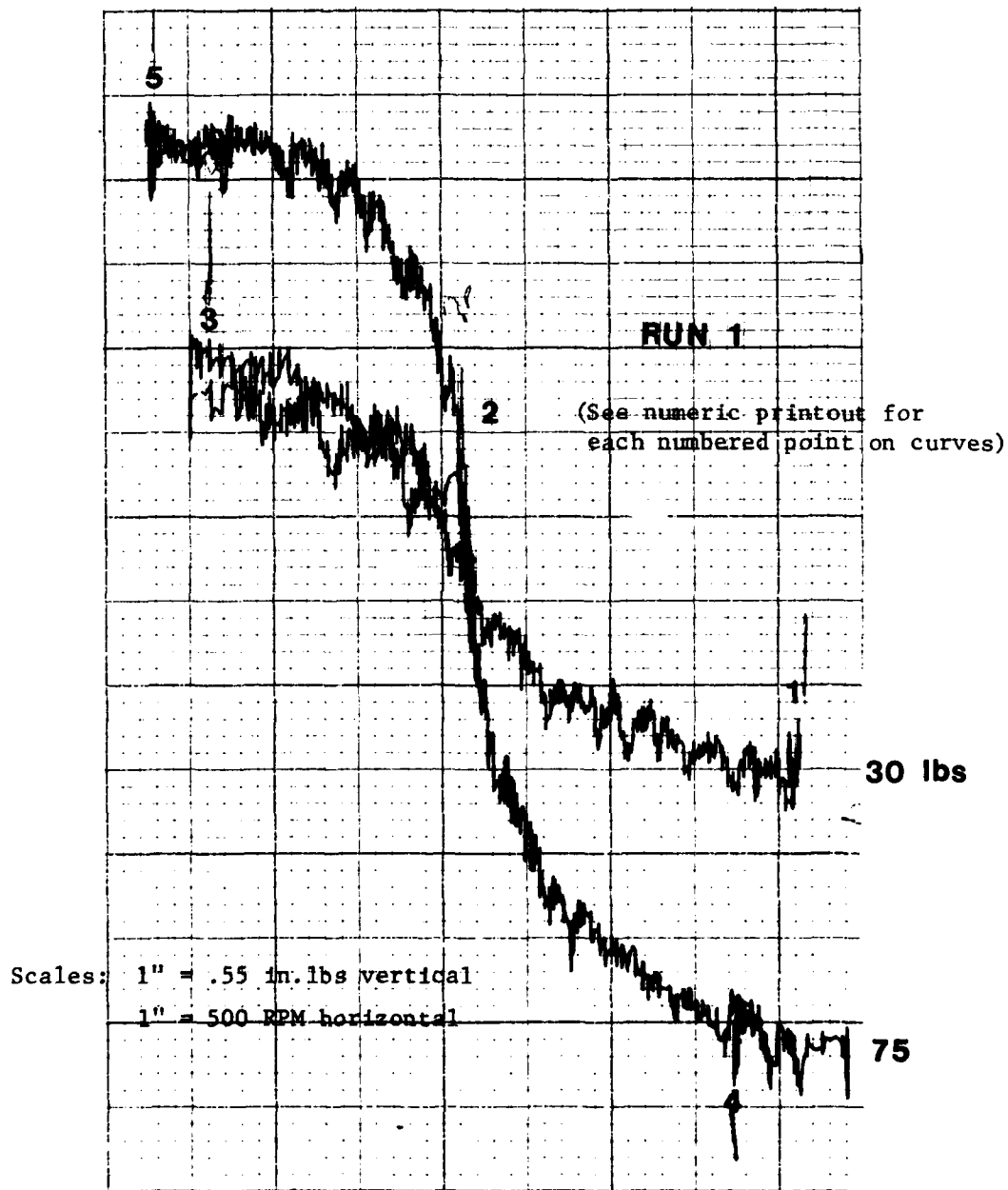


Figure V-6 Run "1" Traction vs. Slip Speed Plot

RUN 2

(See Run of Torque vs. Slip Speed)

9 70.20°F
8 73.20°F
7 81.40°F
6 77.80°F
5 80.60°F (1)
4 80.30°F
3 2064.0RPM
2 -73.42LBS
1 549.5RPM
0 -1.9657TOR
P 261:16:45:03

9 76.80°F
8 72.90°F
7 82.10°F
6 77.60°F
5 79.90°F
4 81.10°F (2)
3 2056.0RPM
2 -71.00LBS
1 -1004.5RPM
0 .27947TOR
P 261:16:45:55

9 71.10°F
8 73.70°F
7 82.70°F
6 78.10°F
5 81.00°F (3)
4 81.80°F
3 2057.0RPM
2 -100.62LBS
1 -807.5RPM
0 .29011TOR
P 261:16:47:01

9 77.60°F
8 73.00°F
7 82.40°F
6 78.30°F
5 81.20°F (4)
4 82.20°F
3 2067.0RPM
2 -98.22LBS
1 755RPM
0 -2.9865TOR
P 261:16:47:46

RUN 2

* See explanation of channel numbers

Figure V-7 Run "2" Data Scanner

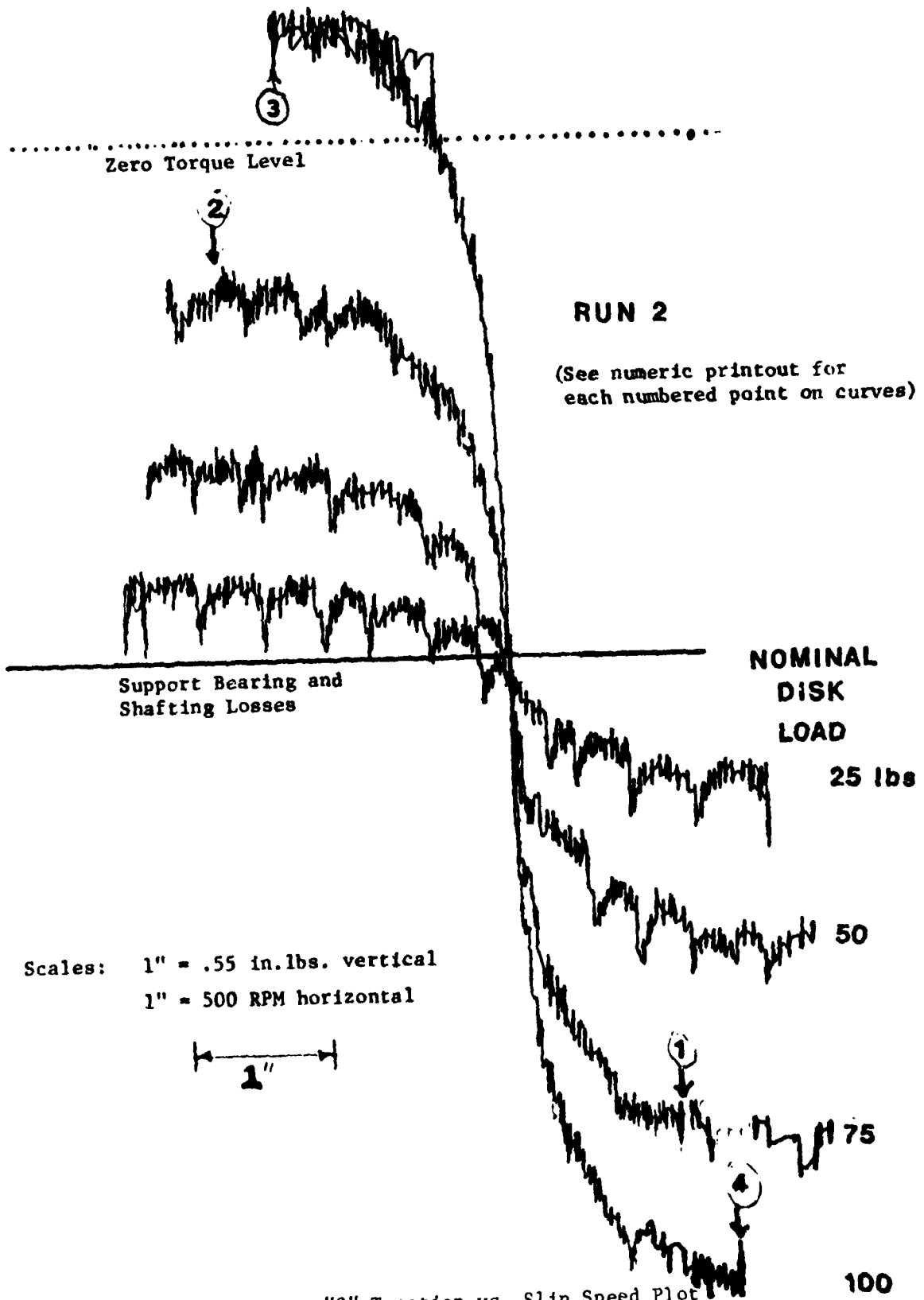


Figure V-8 Run "2" Traction vs. Slip Speed Plot

END